



Review article

Nitrogen-containing heterocyclic drug products approved by the FDA in 2023: Synthesis and biological activity

Weijiang Luo^a, Yiqi Liu^a, Hui Qin^d, Zeyan Zhao^a, Suqi Wang^a, Weimin He^{c,**}, Shengsong Tang^{b,***}, Junmei Peng^{a,*}

^a Department of Medicinal Chemistry, School of Pharmacy, Hengyang Medical School, University of South China, China

^b Hunan Province Key Laboratory for Antibody-based Drug and Intelligent Delivery System, School of Pharmaceutical Sciences, Hunan University of Medicine, China

^c School of Chemistry and Chemical Engineering, University of South China, Hengyang, Hunan, 421001, China

^d Hengyang Medical School, University of South China, Hengyang, Hunan, 421001, China

ARTICLE INFO

Keywords:

Nitrogen-containing heterocyclic drugs

Pharmaceuticals

Synthesis

Medicinal chemistry

Bioactivity

ABSTRACT

This article profiles 13 newly approved nitrogen-containing heterocyclic drugs by the U.S. Food and Drug Administration (FDA) in 2023. These drugs target a variety of therapeutic areas including proteinuria in patients with IgA nephropathy, migraine in adults, Rett syndrome, PI3K δ syndrome, vasomotor symptoms, alopecia areata, acute myeloid leukemia, postpartum depression, myelofibrosis, and various cancer and tumor types. The molecular structures of these approved drugs feature common aromatic heterocyclic compounds such as pyrrole, imidazole, pyrazole, isoxazole, pyridine, and pyrimidine, as well as aliphatic heterocyclic compounds like caprolactam, piperazine, and piperidine. Some compounds also contain multiple heteroatoms like 1,2,4-thiadiazole and 1,2,4-triazole. The article provides a comprehensive overview of the bioactivity spectrum, medicinal chemistry discovery, and synthetic methods for each compound.

1. Introduction

Nitrogen-containing heterocyclic compounds are cyclic compounds that consist of both carbon and nitrogen atoms. Examples of these compounds include pyrrole, imidazole, and pyrazole, all of which contain nitrogen heteroatoms. These nitrogen heterocycles are commonly found in nature, with many natural products and pharmaceutical molecules belonging to this category. They exhibit various pharmaceutical activities such as anti-inflammatory [1], antibacterial [2], and anti-cancer properties [3]. Additionally, nitrogen heterocyclic compounds are extensively used in pesticides like insecticides [4], acaricides [5], and herbicides [6]. An analysis of US FDA-approved drugs by Vitaku et al. [7], revealed that 59 % of small molecule drugs contain nitrogen heterocycles. These compounds are often utilized as anti-tumor agents [8], kinase inhibitors [9], anti-diabetic drugs [10], anti-convulsants [11], anti-inflammatory agents [1,12], antibacterials [13,14], and antidepressants [15]. Compounds discussed in this study include (Fig. 1) JaypricaTM (1), FilspariTM (2), ZavzpretTM (3),

DaybueTM (4), JoenjaTM (5), VeozahTM (6), LitfuloTM (7), VanflytaTM (8), ZurzuvaTM (9), SohonosTM (10), OjjaaraTM (11), TruqapTM (12), OgsiveoTM (13). Most compounds are used to treat a variety of tumors and cancers (1, 8, 12, 13). Other therapeutic disorders include proteinuria in patients with IgA nephropathy (2), migraine in adults (3), Rett syndrome (4), PI3K δ syndrome (5), vasodilatory symptoms (6), pemphigus vulgaris (7), postpartum depression (9), progressive ossifying fibrous dysplasia (10), myelofibrosis with anemia in adults (11).

2. Pirtobrutinib (JaypricaTM)

Pirtobrutinib (1, LOXO-305), a highly selective non-covalent reversible Bruton's tyrosine kinase (BTK) inhibitor developed by Loxo Oncology [16]. The first-generation BTK inhibitor Ibrutinib, approved in 2013, is the most commonly used single drug for MCL. Ibrutinib, along with subsequent BTK inhibitors such as zanubrutinib, tirabrutinib, and orelabrutinib, are covalent BTK inhibitors that exert anti-tumor effects by irreversibly binding to C481 of BTK. Long-term use of these inhibitors

* Corresponding author.

** Corresponding author.

*** Corresponding author.

E-mail addresses: weiminhe@usc.edu.cn (W. He), tangss_submit@163.com (S. Tang), pengmarina@126.com (J. Peng).

may lead to mutations at the C481 site. Pirtobrutinib (**1**) demonstrates similar potency against both wild-type (WT) and C481 mutant BTK. Research by Aishath S Naeem's team indicates that LOXO-305 and ibrutinib have comparable inhibitory activities against wild-type BTK in WT BTK HEK cells, with IC_{50} values of 5.69 nmol/L and 3.33 nmol/L for phospho-BTK inhibition, respectively. Furthermore, LOXO-305 inhibits phospho-BTK in btk-c481s expressed HEK293 cells with an IC_{50} value of 21.2 nmol/L [17].

A Phase 1/2 study of pirtobrutinib (**1**) demonstrated an absolute bioavailability of 85.5 % following a single oral dose of 200 mg. In vitro studies indicate that pirtobrutinib (**1**) is metabolized primarily through direct glucuronidation via CYP3A4, UGT1A8, and UGT1A9. The drug exhibits an effective half-life of approximately 19 h and a mean apparent clearance rate of 2.02 L/h [18]. The most commonly reported adverse reactions included decreased neutrophil count (41 %), decreased platelet count (27 %), and diarrhea (20 %). Pirtobrutinib (**1**) demonstrates greater selectivity for BTK compared to previous-generation BTK inhibitors and binds to the receptor non-covalently. This characteristic makes it a valuable option for treating B-cell malignancies that have become resistant to earlier BTK inhibitors. Pirtobrutinib (**1**) was approved in the USA in January 2023, with the trade name Jayprica™, which was used for the treatment of adults with relapsed and refractory mantle cell lymphoma (MCL) [19].

The synthesis pathway of pirtobrutinib (**1**) is exclusively documented in patents, with Loxo Oncology being the first to propose it [20]. Initially, [(1S)-2,2,2-trifluoro-1-methyl-ethyl]benzoyl hydrazide is utilized as the starting material to synthesize [(1S)-2,2,2-trifluoro-1-methyl base-ethyl]hydrazine. Subsequently, 5-fluoro-2-methoxybenzoic acid is employed as the starting material in a two-step acid chloride reaction followed by a one-step amide reaction to yield the intermediate *N*-[4-(2,2-cyano-hydroxy-Vinyl)phenyl]methyl]-5-fluoro-2-methoxy-benzamide. This intermediate undergoes cyclization with hydrazine and final hydrolysis of the nitrile group to produce pirtobrutinib (**1**). Although this route is used for pirtobrutinib (**1**) synthesis, it is lengthy with low yields. In 2023, Beijing Kanglisheng Pharmaceutical Technology Development Co., Ltd. introduced a high-yield preparation route for pirtobrutinib (**1**). In the reaction scheme depicted in Scheme 1 [21]. First, 4-formylbenzoic

acid methyl ester (**14**) was stirred with hydroxylamine hydrochloride at room temperature for 2 h to produce 4-oximinomethylbenzoic acid methyl ester **15**. Subsequently, **15** was treated with sodium hydroxide and 5 % Pd/C in React at room temperature for 3 h under 5–10 atm to yield 4-aminomethylbenzoic acid **16**. Compound **16** was then reacted with malononitrile to form the intermediate 2-(4-(aminomethyl)benzoyl)malononitrile **17**. This intermediate underwent an acylation reaction with 5-fluoro-2-methoxybenzoic acid (**18**) at 40–50 °C to produce intermediate **19**, which was further reacted with [(1S)-2,2,2-trifluoro-1-methyl-Ethyl]hydrazine hydrochloride (**20**) at 55–60 °C for 14 h to undergo a cyclization reaction, resulting in the formation of intermediate **21**. Finally, the nitrile group of **21** was hydrolyzed with methanesulfonic acid to yield pirtobrutinib (**1**).

3. Sparsentan (Filspari™)

Sparsentan (**2**, RE-021) is an oral dual endothelin-angiotensin (ETA) receptor antagonist developed by Traver Therapeutics [22]. It consists of biphenyl C_2 isoxazole sulfonamide and an imidazole-4-one moiety. Research indicates that the isoxazole sulfonamide positioned at C_2 of the biphenyl core plays a crucial role in ETA receptor activity [23]. Additionally, all AT_1 receptor antagonists feature a hydrogen bond donor heterocycle at C_4 of the biphenyl core (Fig. 2). The Bristol-Myers Squibb Pharmaceutical Research Institute utilized key structural elements from the AT_1 receptor antagonist (**1a**, irbesartan) and the biphenyl sulfonamide ETA receptor antagonist (**1b**) to create a scaffold with potent antagonist activity for both receptors. This new compound, **1c** (Fig. 2), was developed by adding a lactam fragment at the 2' position of the scaffold. **1c** demonstrated strong dual-receptor antagonist activity (AT_1 K_i = 10 nmol/L and ETA K_i = 1.9 nmol/L) but had low oral bioavailability in dogs and monkeys. Subsequent SAR studies on **1c** led to the discovery of sparsentan (**2**) [24], achieved by replacing the lactam fragment with an ethoxymethyl group at the 2' position. Sparsentan (**2**) showed improved oral bioavailability (AT_1 K_i = 0.8 nmol/L and ETA K_i = 9.3 nmol/L) and dose-dependent antagonistic effects on the Ang II-induced pressor response.

At steady state with a dosage of 400 mg once daily, the geometric

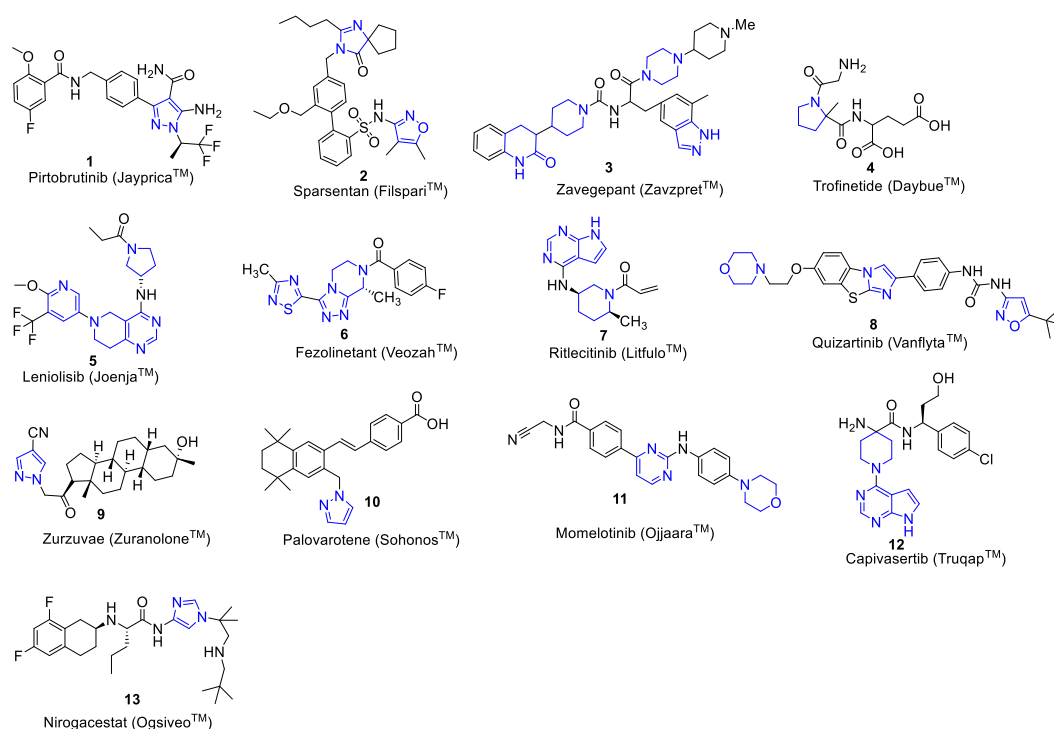
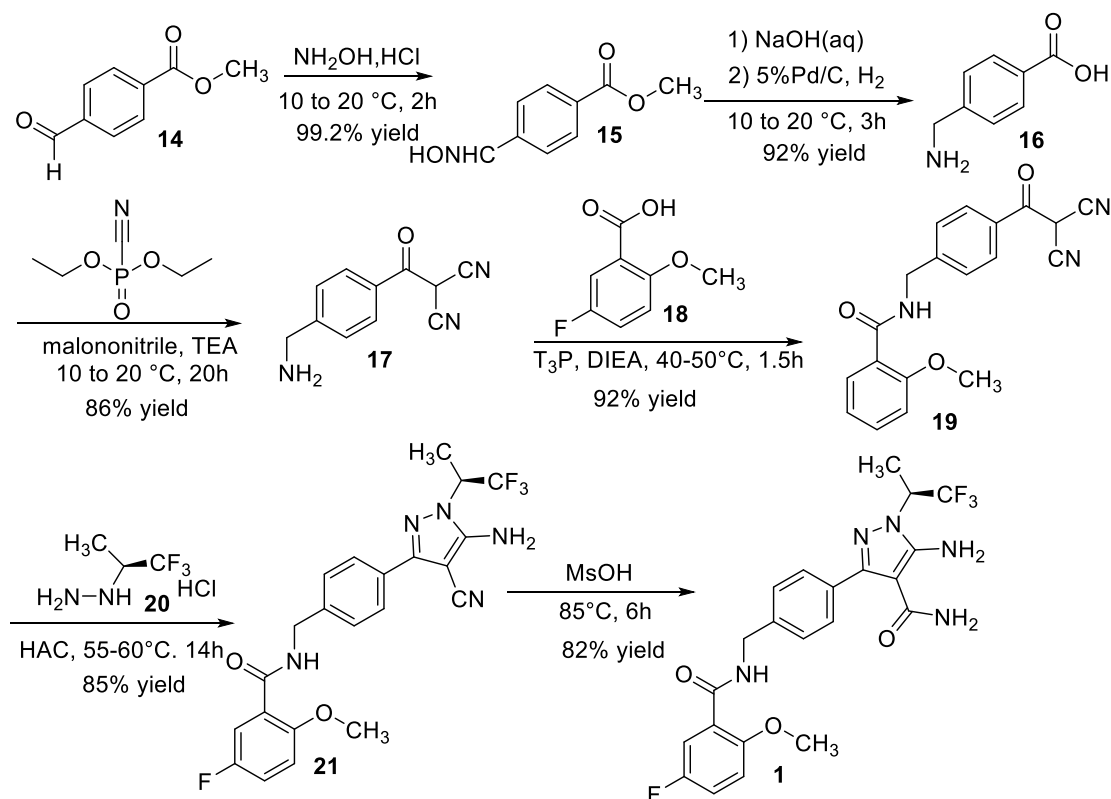


Fig. 1. Nitrogen-containing heterocyclic drugs approved by the US FDA in 2023.



Scheme 1. Synthesis of Pirtobrutinib (1).

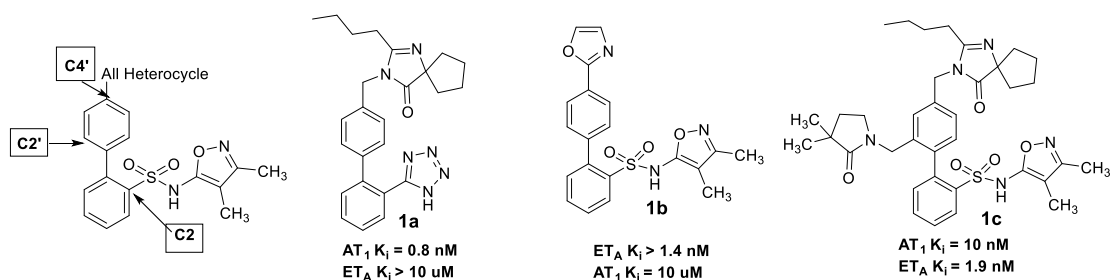


Fig. 2. Structures of 1a, 1b and 1c.

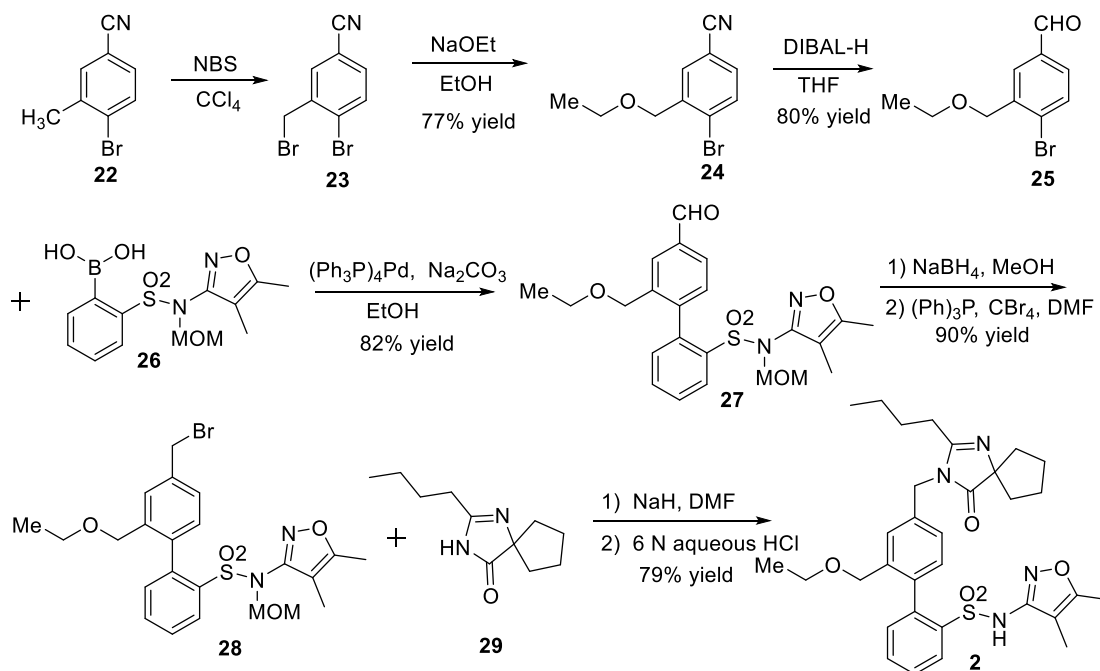
mean values for sparsentan (2) were as follows: maximum concentration (C_{max}) 6.47 $\mu\text{g/mL}$, plasma concentration-time curve 63.6 $\mu\text{g h/mL}$, apparent volume of distribution 61.4 L, and half-life 9.6 h. Sparsentan (2) is predominantly metabolized by CYP3A. In the PROTECT trial involving patients with immunoglobulin A (IgA) nephropathy, the most common adverse reactions to sparsentan (2) included peripheral edema (14 %), hypotension (14 %), and dizziness (13 %) [25]. In comparison to other medications, sparsentan (2) produces a synergistic antihypertensive effect by integrating the essential elements of AT1R and ETAR antagonism. Furthermore, it is the sole non-immunosuppressive drug approved for the treatment of IgA nephropathy. Sparsentan (2) was approved in the USA in February 2023, with the trade name Filspari™, which was used for reducing proteinuria in adult patients with primary IgA nephropathy at risk for rapid disease progression [26].

The synthesis of sparsentan (2) was outlined in Scheme 2 by Trave Therapeutics [24], starting with 4-bromo-3-methylbenzonitrile (22) as the primary material. The process involved treating 4-bromo-3-methylbenzonitrile with *N*-bromosuccinimide to yield bromide 23, followed by a reaction with sodium ethoxide in ethanol to form ethoxymethyl 24. Subsequently, DIBAL was used to reduce the nitrile in 24 to aldehyde 25, which was then coupled with MOM-protected boronic acid 26 using

palladium tetraphenylphosphine as a catalyst to produce biphenyl 27. The aldehyde in 27 was further reduced with sodium borohydride in tetrahydrofuran, tetrabromide to yield bromine 28. The bromine in 28 reacted with the amino group of imidazolinone 29, followed by treatment with aqueous hydrochloric acid. Subsequent deprotection of the MOM group led to sparsentan (2).

4. Zavegepant (Zavzpret™)

Zavegepant (3, BMS-742413) is a third-generation small molecule calcitonin gene-related peptide (CGRP) receptor antagonist developed by Pfizer for the prevention and treatment of chronic and episodic migraine [27]. Initially discovered by the Bristol-Myers Squibb R&D Center, zavegepant (3) contains 1*H*-indazole and 1-(piperidin-4-yl) piperazine heterocycles (Fig. 1). zavegepant (3) is a compound derived from the high-affinity CGRP receptor antagonist 2a (BMS-694153). Dihydroquinazolinone in 2a (BMS-694153) was found oxidative stability in aqueous solution that was accelerated by light and to cause nasal irritation and olfactory epithelial atrophy in rodent toxicity studies. subsequently, Bristol-Myers Squibb [28] made modifications to enhance its stability, replacing the methylene group in 3,



Scheme 2. Synthesis of Sparsentan (2).

4-dihydroquinazolin-2(1H)-one **2a** (position 4) with an ethylene isostere giving a quinolin-2(1H)-one core **2b** from which zavegepant (**3**) was built (Fig. 3). This compound demonstrated a concentration-dependent inhibitory effect on the binding of [¹²⁵I]CGRP to the human CGRP receptor on SK-N-MC cell membranes, with an average K_i of 23 ± 2 pM [29].

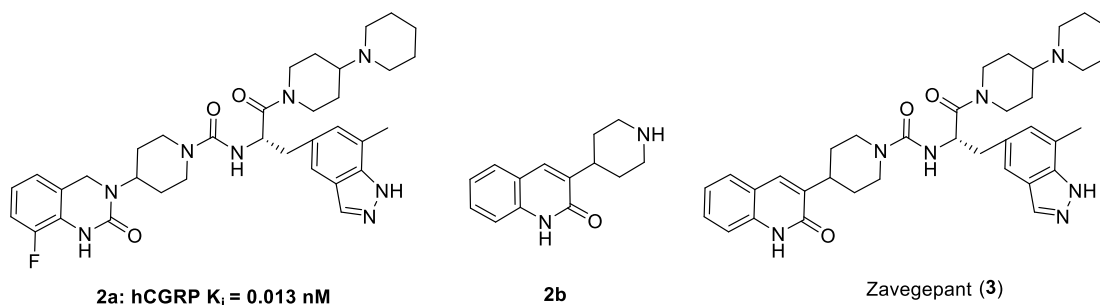
Zavegepant (**3**) administered as a nasal spray is absorbed rapidly, achieving peak blood concentrations approximately 30 min after a single 10 mg dose. The absolute bioavailability of intranasal zavegepant (**3**) is approximately 5 %. In vitro studies indicate that zavegepant (**3**) is primarily metabolized by CYP3A4, with a lesser contribution from CYP2D6. Data from Phase III trials (NCT04571060) revealed that the most common adverse reactions among patients treated with zavegepant (**3**) included dysgeusia (18 %, encompassing both dysgeusia and geriatric), nausea (4 %), and nasal discomfort (3 %) [30]. In comparison to other medications, zavegepant (**3**) deviates from the conventional oral administration route by acting directly on the nasal mucosa. This allows for rapid onset of action while avoiding systemic side effects. Zavegepant (**3**) was approved in the USA in March 2023, with the trade name Zavzpret™, which was used for the treatment of migraine in adults, with or without aura [31].

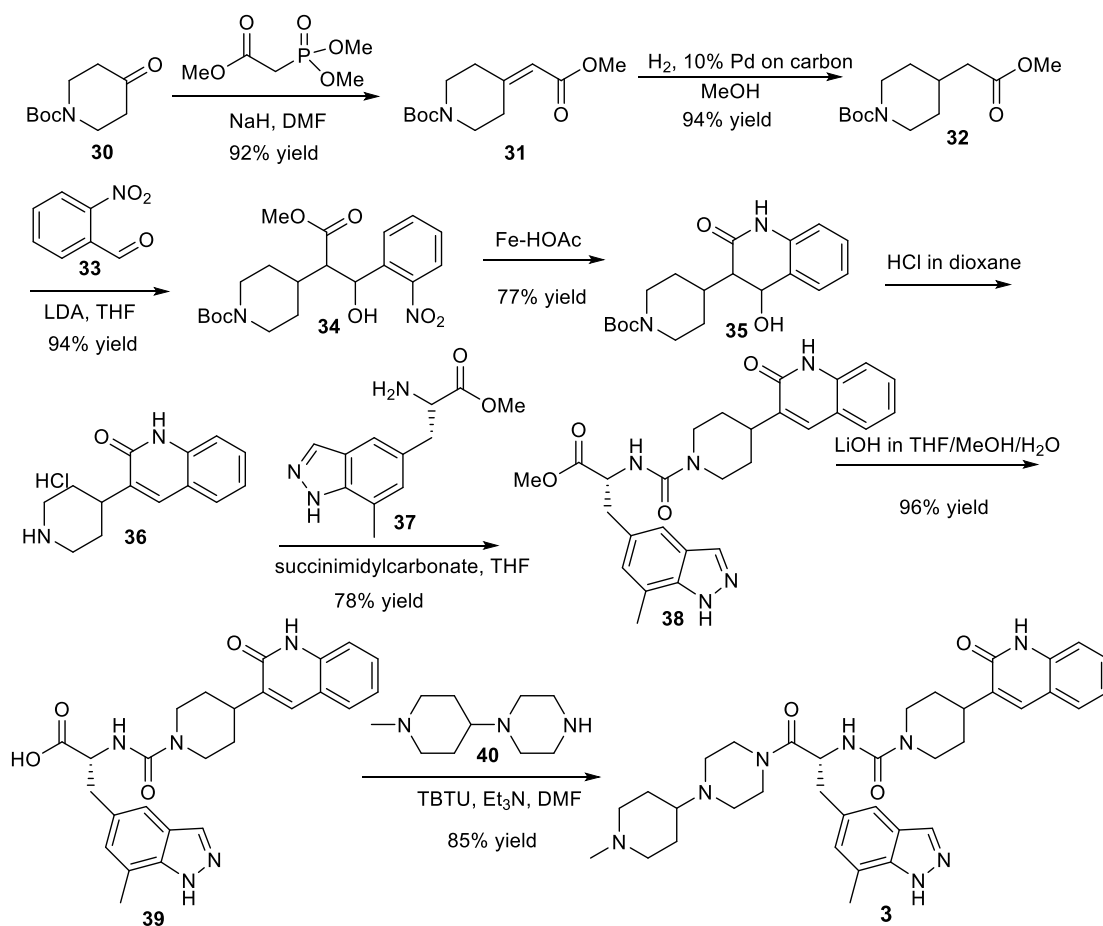
The synthesis method of zavegepant (**3**) is depicted in Scheme 3 [28]. *N*-*boc*-4-piperidone (**30**) underwent the Horner-Emmons reaction with trimethylphosphine acetate to yield an acyl group-containing intermediate **31**, which was subsequently catalyzed by palladium on carbon.

The unsaturated double bond was then reduced through hydrogenation, and the resulting intermediate **32** was treated with LDA to form an enol ester. This enol ester was then reacted with 2-nitrobenzaldehyde **33** to produce nitroalcohol **34** as a diastereomeric mixture. The nitro group of intermediate **34** was further reduced using iron in acetic acid to obtain intermediate **35**, which was then subjected to treatment with hydrogen chloride in dioxane to yield the desired quinolone **36**. Intermediate **36** was effectively coupled with compound **37** using *N,N*-disuccinimidyl carbonate to produce intermediate **38** [32,33]. Subsequently, intermediate **38** was hydrolyzed in a lithium hydroxide solution to obtain carboxylic acid **39**. Following this, intermediate **39** was coupled with 1-(1-methylpiperidin-4-yl)piperazine (**40**) using TBTU to finally synthesize zavegepant (**3**).

5. Trofinetide (DAYBUE™)

Trofinetide (**4**, NNZ-2566), developed by Neuren Pharmaceuticals and Acadia Pharmaceuticals, is utilized for the treatment of the rare Rett syndrome in children. Rett syndrome is a complex neurodevelopmental disorder primarily caused by loss-of-function mutations in the X-linked gene methylated cpb binding protein 2 (MECP2) [34–36]. Trofinetide (**4**) is an orally available small molecule synthetic glycine-proline-glutamate (GPE) analog containing a pyrrolidine heterocycle. GPE is an N-terminal tripeptide endogenously cleaved from insulin-like growth factor-1 in the brain, and is neuroprotective against

Fig. 3. Structures of **2a** and **2b** and zavegepant (**3**).

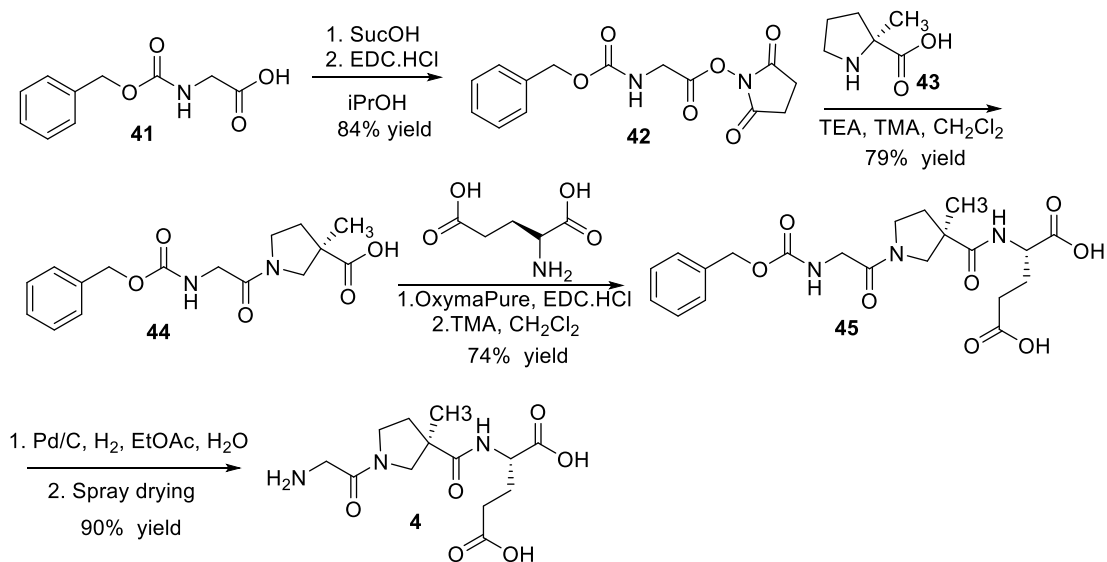


Scheme 3. Synthesis of Zavegepant (3).

hypoxic-ischemic brain injury and neurodegenerative diseases [37,38]. Phase 2 studies of trofinetide (4) demonstrated that 6 weeks of treatment with trofinetide (200 mg/kg twice daily (BID)) was generally well tolerated and provided statistically significant ($P \leq 0.05$) improvements on surface measures of efficacy as assessed by caregivers and clinicians compared to placebo [39].

Phase I studies of trofinetide (4) [40] showed that the

pharmacokinetics of oral trofinetide (4) were linear, exhibiting no time- or dose-dependent effects. Peak concentrations were achieved 2–3 h after oral administration of trofinetide (4), with absorption rates exceeding 84 % following a 12,000 mg dose. The apparent volume of distribution of trofinetide (4) in healthy adults after oral dosing is approximately 80 L. In this population, the effective elimination half-life of oral trofinetide (4) is around 1.5 h. Trofinetide (4) is primarily



Scheme 4. Synthesis of Trofinetide (4).

excreted in the urine as an unchanged drug, accounting for approximately 80 % of the administered dose. In the phase 3 study (NCT04181723) [41], diarrhea was a common treatment-emergent adverse event, occurring in 80.6 % of participants. Trofinetide (4) was approved by the US FDA in March 2023 under the trade name Daybue™ for the treatment of Rett syndrome in adults and children aged 2 years and older [42].

The synthesis of trofinetide (4) is depicted in Scheme 4 and detailed in Neuren Pharmaceuticals' patent [43]. Starting with benzyloxycarbonyl-glycine (41), an esterification reaction with *N*-hydroxysuccinimide in isopropyl alcohol yielded intermediate 42. Subsequent ammonolysis reaction with 43 in dichloromethane produced intermediates 44. These intermediates were activated by OxymaPure and EDC-HCl, followed by acylation with TMA silylated glutamic acid to form intermediate 45. Finally, intermediate 45 underwent hydrogenation with Pd/C and was then spray-dried to yield trofinetide (4).

6. Leniolisib (Joenja™)

Leniolisib (5, CDZ173) was initially identified by Novartis as a potent and selective inhibitor of PI3Kδ [44]. It features a core structure of 5, 6, 7, 8-tetrahydropyrido[4, 3-*d*]pyrimidine (THPP) with a pyridine alkoxy substituent (Fig. 1). Structure-activity relationship (SAR) studies [45] revealed that replacing quinazoline 3a (HT-logP = 2.7) with THPP skeleton 3b (HT-logP = 0.7) significantly decreased its lipophilicity (Fig. 4). The introduction of the pyridine alkoxy substituent into the THPP core enhances PI3Kδ activity in the cell and therefore preserves its structure. Moreover, the addition of a CF₃ group at the 3-position of methoxypyridine increased the potency of PI3Kδ by fivefold, with an IC₅₀ value of 11 nmol/L. Leniolisib (5) exhibits IC₅₀ (μmol/L) values of 0.244, 0.424, 2.23, and 0.011 against PI3Kα, PI3Kβ, PI3Kγ, and PI3Kδ, respectively.

The C_{max} and area under the curve (AUC) values for leniolisib (5) increased proportionally across the 20–140 mg twice-daily dosing range. Following both single and multiple ascending doses of leniolisib (5), C_{max} was attained approximately 1 h post-dose. Leniolisib (5) was extensively metabolized by the liver, primarily through CYP3A4, with lesser contributions from CYP3A5, CYP1A2, and CYP2D6 [46]. Data from the Phase II/III study (NCT02435173) [47] indicated that the most common adverse reactions in the leniolisib (5) group included headache (24 %), sinusitis (19 %), and atopic dermatitis (14 %). Compared to the reliance on antibiotics and immunoglobulin replacement therapy, leniolisib (5), as the first oral targeted therapy, offers advantages such as good efficacy and minimal side effects. Leniolisib (5) was approved in the USA in March 2023, with the trade name Joenja™, which was used for the treatment of activated PI3Kδ syndrome (APDS) in adult and pediatric patients aged 12 years and above [48].

The synthesis of leniolisib (5) was first reported in a Novartis patent [49]. In the reaction scheme depicted in Fig. 5. Initially, starting materials such as 6-benzyl-4-chloro-5, 6, 7, 8-tetrahydropyrido[4, 3-*d*]pyrimidine (4a), (*S*)-3-aminopyrrolidine-1, *tert*-butyl formate (4b), 5-bromo-2-methoxy-3-(trifluoromethyl)pyridine (4c), and propionyl chloride (4d) were used in a 5-step reaction to produce leniolisib (5). However, this method was found to be time-consuming and resulted in

lower overall yield. Subsequently, Kangli Company [50] improved the synthesis of leniolisib (5) by utilizing 4-chloro-5, 6, 7, 8-tetrahydropyrido[4, 3-*d*]pyrimidine (46) as a raw material (Scheme 5). *N*-arylation of 46 and 47 at 100 °C yielded intermediate 48 in 60 % yield, which was then reacted with (*S*)-1-(3-aminopyrrolidin-1-yl)propan-1-one (49) at 120 °C for 24 h to obtain leniolisib (5) with 76 % yield.

7. Fezolinetant (Veoza™)

Fezolinetant (6, ESN-364) is an oral, small molecule neurokinin 3 receptor (NK3R) antagonist developed by Astellas Pharma Inc. NK3R is a key regulatory component of the hypothalamic-pituitary-gonadal (HPG) axis, where its activation actively regulates gonadotropin-releasing hormone (GnRH) pulse frequency [51]. Fezolinetant (6) is composed of an *N*-acyltriazolepiperazine core domain, a methylthiadiazole ring, and a monofluorinated phenyl fragment (Fig. 1). Structure-activity relationship (SAR) studies conducted by Hamid R. Hoveyda [52] demonstrated fezolinetant's potency against human NK3R (K_i = 21.8 nmol/L). Furthermore, fezolinetant (6) exhibits more than 450-fold selectivity for human NK3R over NK1 and NK2 receptors [53].

The C_{max} and AUC increased linearly with escalating doses in healthy females receiving fezolinetant (6) at 20–60 mg once daily. The median time to reach C_{max} was 1.5 h, and the mean apparent volume of distribution was 189 L. The effective half-life for alleviating vasomotor symptoms (VMS) in women was 9.6 h. Fezolinetant (6) is primarily metabolized by cytochrome P450 (CYP) 1A2, with CYP2C9 and CYP2C19 contributing to a lesser extent. A safety study of fezolinetant (6) in the treatment of menopausal vasodilatory symptoms indicated that the most common treatment-emergent adverse event was headache, occurring in 9.0 % of participants [54]. In comparison to hormonal therapies, fezolinetant (6) represents the world's first non-hormonal targeted treatment for VMS. It is associated with fewer and less severe side effects, offers a broader range of applications, and provides significant therapeutic advantages. Fezolinetant (6) got its first approval by the US FDA in May 2023 under the trade name Veoza™ for the treatment of moderate to severe VMS or hot flashes caused by menopause [55].

The synthesis of fezolinetant (6) developed by the Hoveyda group is illustrated in Scheme 6 [56]. The synthesis started with the use of acid 50 with the methyl esterifying reagent diazomethane to produce ester 51. 51 was reacted with hydrazine to produce the key intermediate hydrazide 52. The amino group of the feedstock ketopiperazine (53) was then protected by DMB (54) to give intermediate 55, which was reacted with freshly prepared triethylhydrazinium fluoroborate for 1 h to give the imino ether 56. 56 Stirring with the key intermediate hydrazide 52 at 55 °C–70 °C for 6 h–8 h afforded intermediate 57, which following removal of the DMB group gave intermediate 58. Finally, intermediate 58 was acylated with 4-fluorobenzoyl chloride (59) at 0 °C to afford fezolinetant (6).

8. Ritlecitinib (Litfulo™)

Ritlecitinib (7) a potent oral JAK3 kinase inhibitor developed by Pfizer, is currently in development for the treatment of alopecia areata [57], vitiligo [58], ulcerative colitis [59], and Crohn's disease [60].

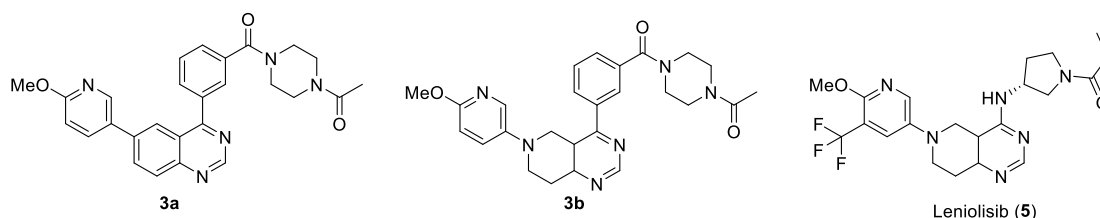


Fig. 4. Structures of 3a, 3b and leniolisib (5).

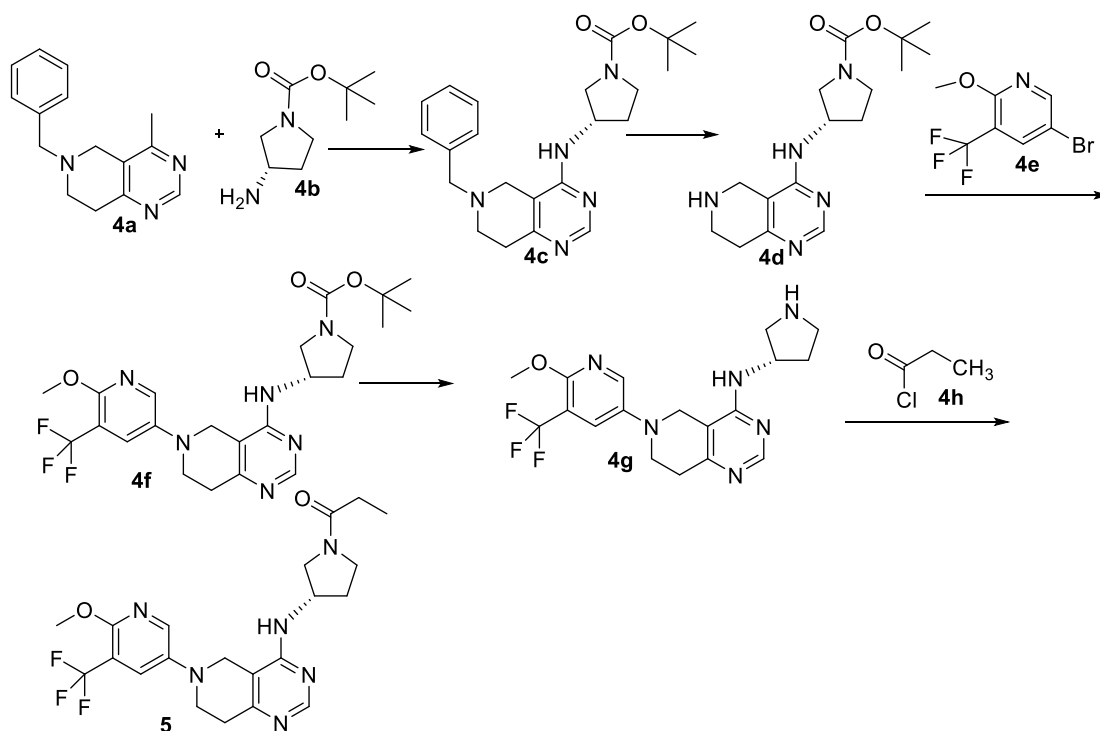
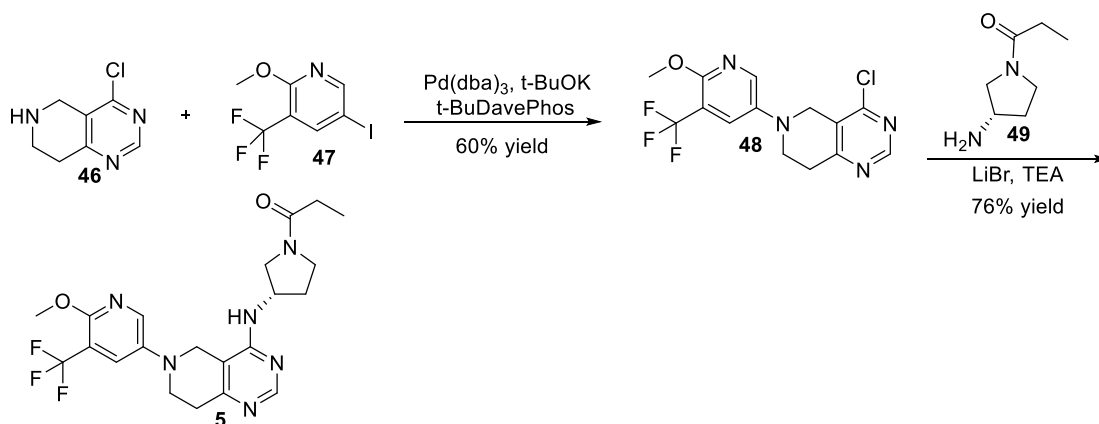


Fig. 5. 5-Step reaction for the synthesis of Leniolisib (5).



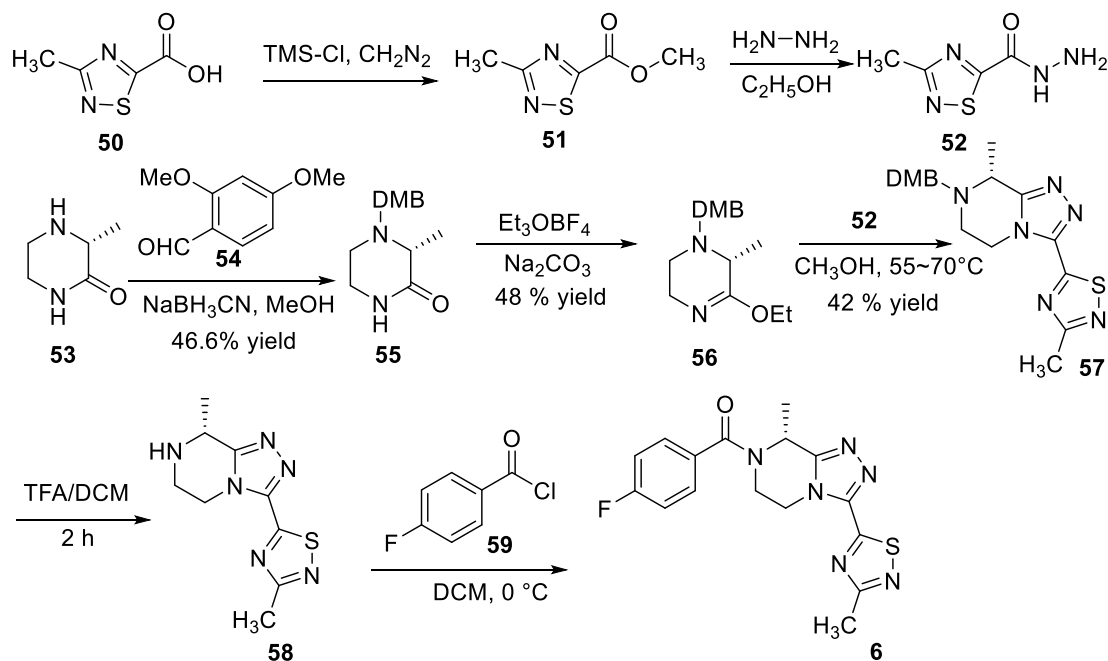
Scheme 5. Synthesis of Leniolisib (5).

Ritlecitinib (7) features two (R) configuration tertiary carbon centers, along with pyrrolopyrimidine and piperidine rings (Fig. 1). Pfizer's structure-activity relationship (SAR) studies have shown that ritlecitinib (7) is a highly specific JAK3 inhibitor ($IC_{50} = 33$ nmol/L) with minimal activity against other JAK enzymes at a concentration of 1 mM ATP. X-ray crystallography has revealed its covalent binding to Cys-909.27 ($IC_{50} = 51$ nmol/L) and its efficacy in human whole blood assay (IL-15 stimulated HWB assay $IC_{50} = 197$ nmol/L) [61]. Structural modifications, such as changing the configuration from R, R to S, S (5c) or R, S (5a, 5b), or altering the methyl position (5d), have been shown to reduce their activity (Fig. 6).

The AUC and the C_{max} of ritlecitinib (7) increased in an approximately dose-proportional manner up to 200 mg, achieving steady state in approximately 4 days. C_{max} was reached within 1 h after the oral administration. The absolute oral bioavailability of ritlecitinib (7) is approximately 64 % [62]. Ritlecitinib (7) undergoes multiple metabolic pathways, including those mediated by glutathione S-transferase (GST), specifically GST A1/3, M1/3/5, P1, S1, T2, Z1, and microsomal GST

1/2/3, as well as cytochrome P450 (CYP) enzymes, including CYP1A2, CYP2C8, CYP2C9, and CYP3A. Interim results from the ALLEGRO-LT study [63] indicated that the most common treatment-emergent adverse event (AE) in patients with pemphigus vulgaris treated with ritlecitinib (7) was headache, occurring in 16 % of patients. The advantages of ritlecitinib (7) over other non-selective JAK inhibitors include the avoidance of cholesterol and liver enzyme elevations associated with the inhibition of JAK1/JAK2, as well as the prevention of thrombocytopenia and anemia resulting from JAK2 inhibition. Ritlecitinib (7) was approved in the USA in March 2023, with the trade name Litfulo™, which was used for the treatment of severe alopecia areata in adults and adolescents over 12 years old [64].

The synthesis of ritlecitinib (7), as illustrated in Scheme 7, was developed by Pfizer [61]. Using 6-methylpyridin-3-amine (60) as the starting material. Initially, the amino group was protected as the Boc derivative in an aqueous solution of tetrahydrofuran and ammonium chloride, utilizing both phases of ethanol to yield intermediate 61. The subsequent reduction of the pyridine ring was conducted using 5 %



Scheme 6. Synthesis of Fezolinetant (6).

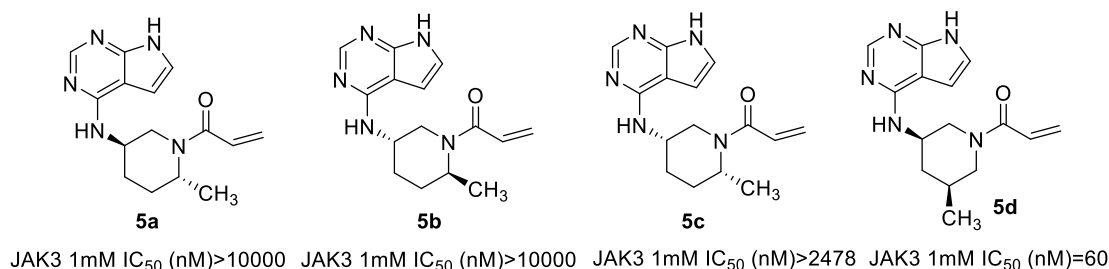


Fig. 6. Structures of 5a, 5b, 5c and 5d.

Rh/C as a catalyst in a solvent mixture of 9:1 ethanol/acetic acid, resulting in intermediate **62**, which was obtained as a *cis/trans* diastereomeric mixture in a ratio of 2.8:1. A slow addition of intermediate **62** to an ethanolic solution of (*R*)-2-(3,5-dinitroanilino)-2-phenylacetic acid at 70 °C produced intermediate **63**. The reaction of **63** with aqueous NaOH in MTBE yielded *cis*-**64**. Treatment of *cis*-**64** with benzyl chloroformate in the presence of NaHCO₃ afforded intermediate **65**. The placement of **65** in excess HCl in methanol, using isopropyl acetate as the solvent, facilitated the removal of the *N*-Boc group, resulting in intermediate **66**. Intermediate **66** was then reacted with **67** in a 5:1 (v/v) mixture of water and MIBK under biphasic S_NAr reaction conditions to produce intermediate **68**. A reduction reaction involving **68**, utilizing 10 % Pd(OH)₂/C as a catalyst and water as the solvent at 80 °C under a hydrogen pressure of 50 psi, yielded intermediate **69**. The subsequent acylation of **69** with 3-chloropropionyl chloride in a tetrahydrofuran/water solvent system resulted in intermediate **70**. Finally, intermediate **70** was reacted with NaOH at 20 °C for approximately 20 h to obtain ritlicitinib (**7**).

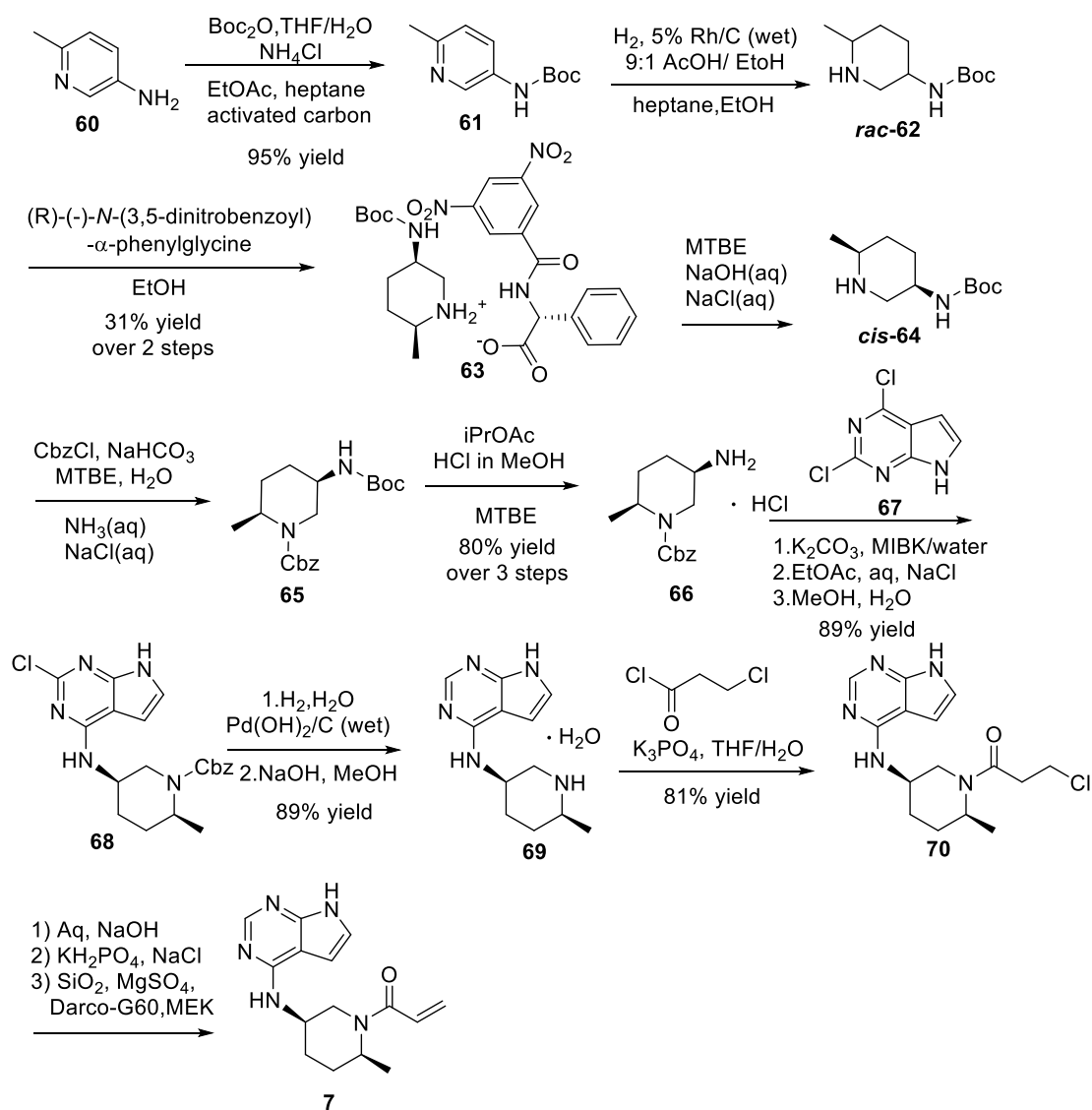
9. Quizartinib (Vanflyta™)

Quizartinib (**8**, AC220) is a FLT3 gene inhibitor developed by Daiichi Sankyo for treating patients with FLT3-ITD acute myeloid leukemia (AML) [65]. AML is a heterogeneous hematopoietic progenitor cell cancer [66]. Quizartinib (**8**) consists of an imidazole benzothiazole ring and a 2-morpholinoethoxy group (Fig. 1). Structure-activity relationship

(SAR) [67] studies indicate that the 2-morpholinoethoxy group at position 7 of the imidazole benzothiazole ring exhibits the most favorable performance, with a binding constant of 1.6 nmol/L and an IC₅₀ of 0.56 nmol/L in MV4-11 cells. The presence of 2-(piperidin-1-yl)ethoxy (**6a**) and 3-morpholinopropoxy groups (**6b**) led to decreased activity, with IC₅₀ (nmol/L) values of 0.88 and 0.79, respectively [68] (Fig. 7). Hu et al. research revealed that quizartinib (**8**) targets FLT3 (ITD/WT) with an IC₅₀ value of (1.1/4.2) nmol/L, demonstrating 10 times higher selectivity for FLT3 compared to KIT, PDGFRα, PDGFRβ, RET, and CSF-1R [69].

Quizartinib (**8**) exposure, as measured by C_{max} and AUC, increased in a dose-dependent manner within the dosage range of 30–60 mg. Quizartinib (**8**) is primarily metabolized by CYP3A4 [70]. In a phase III study (NCT02668653) [71], the most frequently observed grade 3 or 4 adverse events included febrile neutropenia, hypokalemia, and pneumonia. Quizartinib (**8**) is an oral, selective second-generation type II FLT3 inhibitor. In comparison to first-generation, non-specific FLT3 inhibitors, it exhibits reduced off-target toxicity, enhanced efficacy, and greater specificity. Quizartinib (**8**) was approved by the US FDA in July 2023 under the trade name Vanflyta™ for the treatment of newly diagnosed AML in adult patients with FLT3-ITD positive test results [72].

The synthesis method of quizartinib (**8**) developed by Daiichi Sankyo is illustrated in Scheme 8 [67]. Initially, 2-amino-6-hydroxybenzothiazole (**71**) and 2-bromo-4-nitroacetophenone (**72**) underwent condensation in refluxing ethanol, leading to the formation of intermediate **73**.



Scheme 7. Synthesis of Ritlecitinib (7).

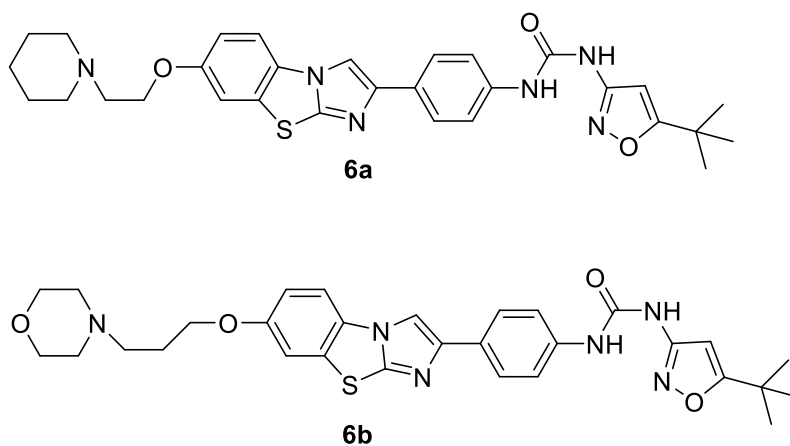
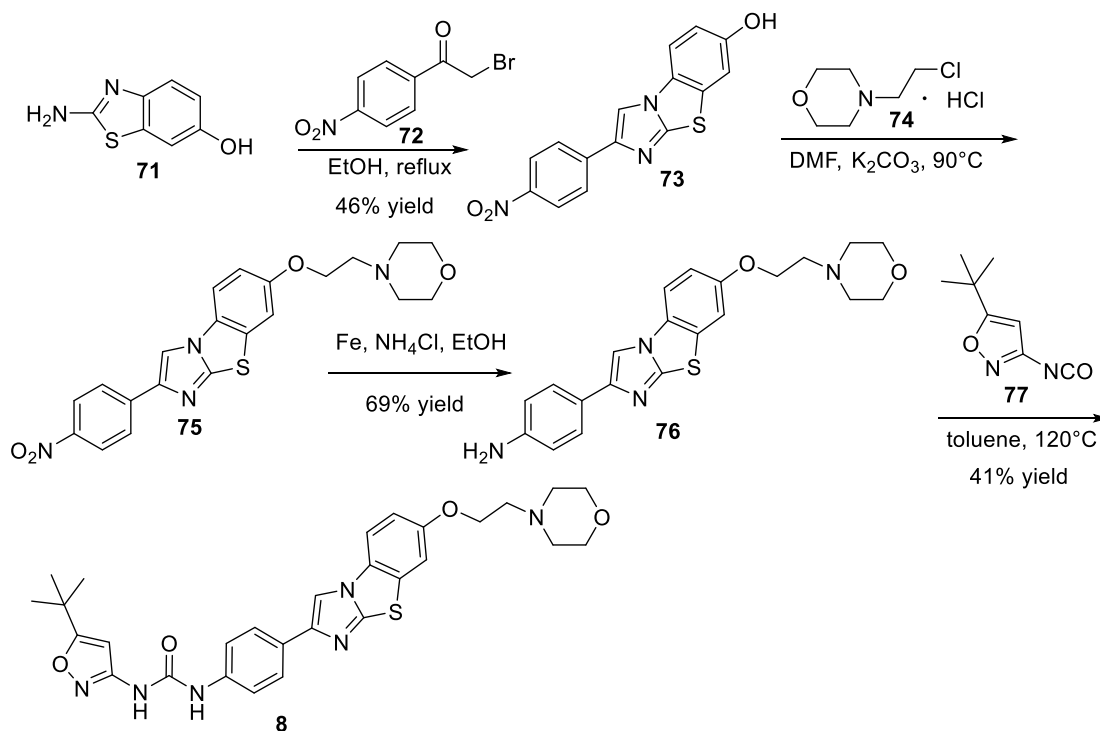


Fig. 7. Structures of 6a and 6b.

The intermediate **73** was reacted with 4-(2-chloroethyl)morpholine hydrochloride (**74**) to form the ether **75** in the presence of DMF and K_2CO_3 . The nitro group of **75** was then reduced with iron powder and ammonium chloride in ethanol to yield the corresponding amine **76**.

Finally, **76** was coupled with 5-*tert*-butyloxazole-3-isocyanate (**77**) in toluene at 120°C to obtain quizartinib (**8**).



Scheme 8. Synthesis of Quizartinib (8).

10. Zuranolone (zurzuvaTM)

Zuranolone (9) is an oral neuroactive steroid and positive allosteric modulator of the gamma-aminobutyric acid alpha (GABA) receptor [73]. GABA is the main inhibitory neurotransmitter in the central nervous system (CNS) and plays a key role in maintaining the balance of neuronal activity in the brain [74]. Zuranolone (9) is composed of a progesterone scaffold with a pyrazole fragment (Fig. 1). SAR studies reported by Botella et al. [75] has indicated that the addition of a specific heterocyclic ring at the C-21 position of the progesterone structure enhances its suitability for oral administration while maintaining its modulatory effect on the GABA receptor. Initially, the inclusion of a triazole ring (7a) (Fig. 8) was found to enhance its interaction with GABA receptors, but subsequent analysis revealed some suboptimal cross-reactivity at certain sites. Ultimately, the incorporation of a 4-cyanopyrazole heterocycle was identified to exhibit improved functional activity on $\alpha 1\beta 2\gamma 2$ (EC₅₀ 375 nmol/L) and $\alpha 4\beta 3\delta$ (EC₅₀ 299 nmol/L) GABA receptors.

In the dose range of 30–60 mg (1.2 times the maximum recommended dose), the C_{max} and the AUC of zuranolone (9) increased in an approximately dose-proportional manner. Zuranolone (9) reaches its C_{max} 5–6 h after oral administration. It is highly bound to plasma proteins (>99.5 %), and the volume of distribution following oral administration exceeds 500 mL [76]. Zuranolone (9) is primarily metabolized

by CYP3A4. Double-blind phase III clinical trials [77] have demonstrated that the most common treatment-emergent adverse events (TEAEs) were headache (14.2 %) and somnolence (11.9 %). Zuranolone (9), as the second drug approved for the treatment of postpartum depression (PPD), offers the advantages of oral administration in outpatient settings and a rapid onset of action when compared to the previously established drug, brexanolone. Zuranolone (9) was approved by the US FDA in August 2023 under the trade name zurzuvaTM for the treatment of postpartum depression in adults [78].

The synthesis method of Zuranolone (9), developed by Sage Therapeutics and Biogen, is illustrated in Scheme 9 [75]. Starting with raw material 78, hydrogenation with palladium in tetrahydrofuran and concentrated hydrobromic acid yielded intermediate 79. Subsequently, the aluminum-based ligand MAD facilitated a methyl Grignard addition on the ketone, introducing 3 β -methyl with excellent stereo- and regioselectivity to obtain intermediate 80. Homologated methyl ketone 83 was prepared from ketone 80 via Wittig reaction followed by hydroboration/oxidation to alkene 81 to afford alcohol 82 which was subsequently oxidized using PCC. Addition of bromine dropwise to intermediate 83 in an HBr solution facilitated alpha bromination of the ketone, yielding intermediate 84. Finally, intermediate 84 underwent a reaction with ethyl 1*H*-pyridine-azole-4-carbonitrile (85) and K₂CO₃ in THF to obtain Zuranolone (9).

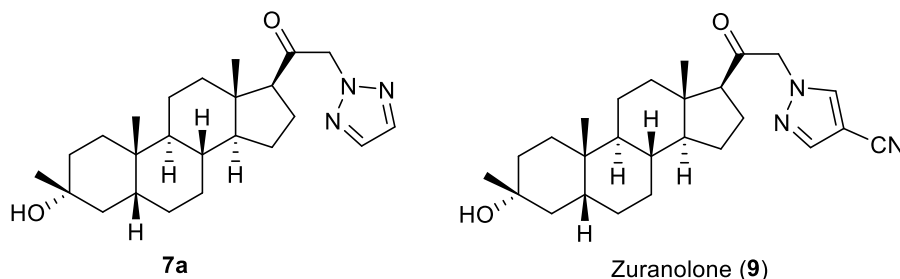
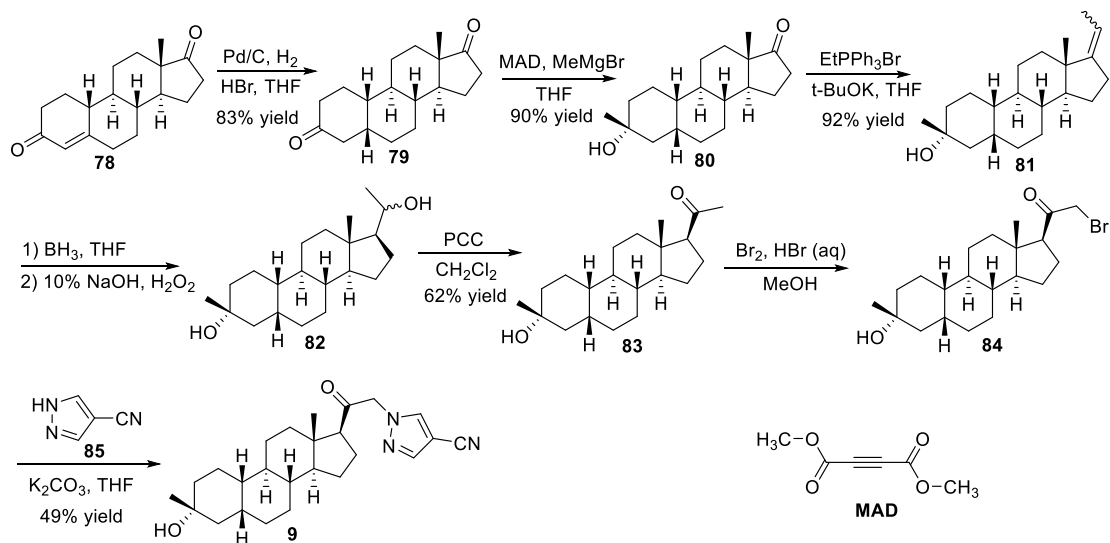


Fig. 8. Structures of 7a and zuranolone (9).



Scheme 9. Synthesis of Zuranolone (9).

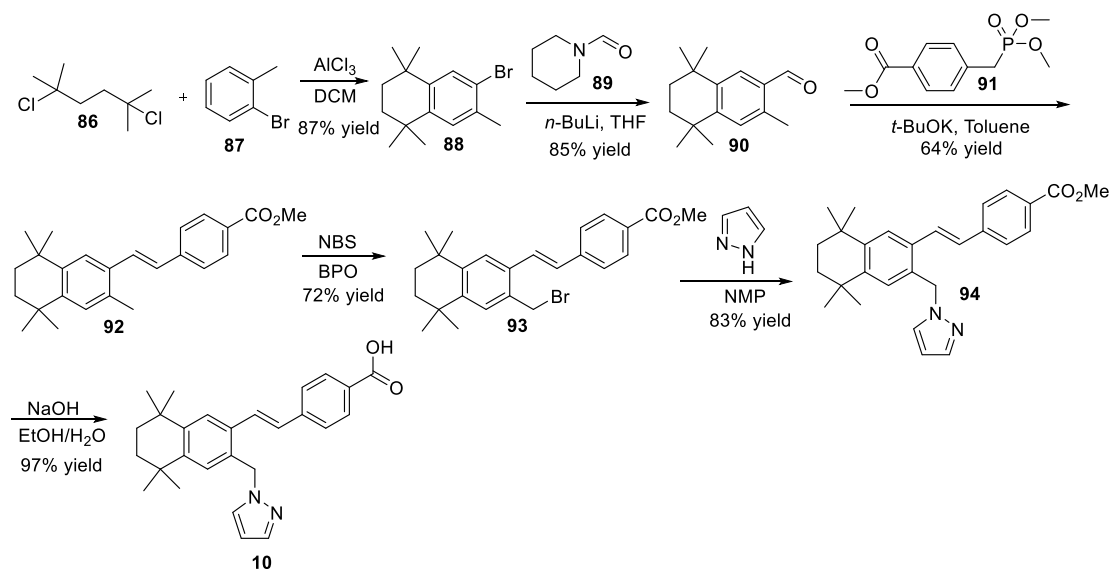
11. Palovarotene (Sohonos™)

Palovarotene (**10**) is an oral selective retinoic acid receptor (RAR) gamma agonist developed by Ipsen to reduce the formation of heterotopic ossification (HO) in patients with fibrodysplasia ossificans progressiva (FOP). FOP is a rare autosomal dominant disorder caused by mutations in the ACVR1/ALK2 gene encoding activin, a receptor type I/activin-like kinase 2 [79], characterized by cartilage formation in ligaments, joints, muscles, and tendons [80,81]. Individuals with FOP have a reduced life expectancy, with an average of about 56 years. By binding to RAR γ , palovarotene (**10**) inhibits bone morphogenetic protein and SMAD 1/5/8 signaling. Interfering with these pathways can prevent cartilage formation, ultimately allowing HO to occur by enabling normal muscle tissue repair or regeneration [82].

The pharmacokinetics of palovarotene are linear and dose-proportional across the dose range of 0.02–50 mg. Patients with fibrodysplasia ossificans progressiva (FOP) reach the maximum concentration of palovarotene (**10**) 3 h after dosing. In vitro studies indicate that palovarotene binds to proteins with a mean binding rate of 99.0 %. It is extensively metabolized by CYP3A4, with lesser contributions from

CYP2C8 and CYP2C19. Caution is advised when administering palovarotene (**10**) to patients with moderate hepatic impairment. Phase II and III studies revealed that the most common adverse reaction associated with palovarotene (**10**) is dry skin, reported in 78 % of patients [83]. Palovarotene (**10**) was approved by the U.S. FDA in August 2023 under the trade name Sohonos™ for reducing novel cancers in adults and children with FOP in women 8 years and older and men 10 years and older, by reducing ossification volume.

The synthesis of Palovarotene (**10**) was initially documented by Roche in a patent, depicted in Scheme 10 [84]. The process began with the Friedel-Crafts alkylation reaction between 2,5-dichloro-2,5-dimethylhexane (**86**) and 2-bromotoluene (**87**), yielding intermediate **88**. Lithium halogen exchange on **88** and formyl transfer using piperidine formamide **89**, gave aldehyde **90**. Compound **90** was then subjected to a Wittig reaction to generate alkene **92**. This in turn underwent radical bromination to form benzyl bromide **93**, which was further reacted with Pyrazole in an S_N2 fashion to yield intermediate **94**. Finally, saponification of ester of **94** provided Palovarotene (**10**).



Scheme 10. Synthesis of Palovarotene (10).

12. Mometotinib (Ojjaara™)

Mometotinib (**11**) is an oral inhibitor of Janus kinase 1 and 2 (JAK1/JAK2) [85] and activin A receptor type I (ACVR1) developed by Gilead Sciences, Inc. It is specifically designed to treat myelofibrosis (MF), a progressive, chronic, Philadelphia chromosome-negative myeloproliferative malignancy associated with activation of the Janus kinase, signal transduction, and activation of transcription (JAK-STAT) pathway [86, 87]. Mometotinib (**11**) consists of a phenylaminopyrimidine core heterocycle and a morpholine fragment. The compound demonstrates potent inhibitory activity against JAK1 (IC_{50} = 11 nmol/L) and JAK2 (IC_{50} = 18 nmol/L). A structure-activity relationship (SAR) study conducted by Burns et al. revealed the crucial role of the morpholine fragment in the compound's inhibitory effects. Replacement of the morpholine fragment with piperazine (**8a**) or thiomorpholine (**8b**) resulted in decreased inhibitory activity (Fig. 9) [88].

Mometotinib (**11**) exposure (C_{max} and AUC) was dose proportional in the 100–300 mg dose range. At steady state, the mean C_{max} of mometotinib (**11**) administered at a dose of 200 mg once daily was 479 ng/mL, with a mean apparent volume of distribution of 984 L. Additionally, the plasma protein binding of mometotinib (**11**) was approximately 91 % in healthy volunteers [89]. Mometotinib (**11**) is metabolized in the liver by several cytochrome P450 (CYP) enzymes, including CYP3A4 (36 %), CYP2C8 (19 %), CYP2C9 (17 %), CYP2C19 (19 %), and CYP1A2 (9 %). The phase III MOMENTUM trial [90] revealed that the most common fatal adverse reaction associated with mometotinib (**11**) was viral infection, occurring in 5 % of cases. Compared to earlier JAK inhibitors, mometotinib (**11**) is the first treatment approved for patients with MF-related anemia, effectively alleviating systemic symptoms and splenomegaly. Mometotinib (**11**) was approved by the US FDA in September 2023 under the trade name Ojjaara™ for the treatment of adults with moderate to high risk MF-related anemia, including primary MF or secondary MF (polycythemia vera and essential thrombocythemia) [91].

The synthesis of mometotinib (**11**) was initially described in a patent by YM BioSciences, illustrated in Scheme 11. As expected, the Suzuki cross-coupling reaction between boronic acid **96** and dichloropyrimidine **95** gave selectively the 4-aryl substituted pyrimidine derivative **97**. The remaining chlorine atom in pyrimidine intermediate **97** was subjected to a nucleophilic aromatic substitution reaction with 4-morpholino-aniline affording intermediate **99**. The cyano group of intermediate **99** was then hydrolyzed using LiOH to form carboxylic acid **100**. Intermediate **100** was activated with HOBt and underwent an acylation reaction with 2-aminoacetonitrile to ultimately generate mometotinib (**11**).

13. Capivasertib (Truqap™)

Capivasertib (**12**, AZD5363) is an oral, small molecule pan-Akt inhibitor developed by AstraZeneca for the treatment of various cancers, including breast [92] and prostate [93] cancer. Capivasertib (**12**) is a chiral compound featuring a tertiary carbon center with *S*-configuration,

a pyrrolo-pyrimidine heterocycle, and a piperidine fragment (Fig. 1). Benzylamide (**9a**) (Fig. 10) has been identified as an orally bioavailable Akt inhibitor, with reported IC_{50} values of 13 nmol/L for Akt1, 66 nmol/L for Akt2, and 57 nmol/L for Akt3, with the IC_{50} value for MDAMB468 cell line is 328 nmol/L [94]. AstraZeneca conducted SAR studies on Benzylamide (**9a**) and discovered that amide α -alkyl substitution can enhance lipophilicity. The ethanol *S*-enantiomer has been identified as a promising substituent, which facilitated the development of capivasertib (**12**). Capivasertib (**12**) exhibits potent pan-Akt enzyme inhibitory effects, with IC_{50} values of 3 nmol/L for Akt1, 8 nmol/L for Akt2, and 8 nmol/L for Akt3, along with the IC_{50} value for MDAMB468 cell line is 89 nmol/L [95].

Capivasertib (**12**) exposure (C_{max} and AUC) is approximately dose proportional in the 80–800 mg dose range [96]. The C_{max} typically reached approximately 1–2 h post-dosing, with an absolute bioavailability of 29 %. The half-life of capivasertib (**12**) is 8.3 h. The metabolism of the drug is primarily mediated by CYP3A4 and UGT2B7. Data from the Phase III CAPItello-291 trial [92] indicated that the most common adverse events observed in the capivasertib (**12**) + fluvastatin group included diarrhea (incidence 72.4 %), rash (38.0 %), nausea (34.6 %), fatigue (20.8 %), and vomiting (20.6 %). Compared to fulvestrant alone, the combination of capivasertib (**12**) and fulvestrant exhibits a significant effect on patients with HER2-negative advanced breast cancer, markedly extending both the median progression-free survival (PFS) and overall survival (OS) of these patients. Capivasertib (**12**), under the trade name Truqap™, was initially approved in the US FDA in November 2023 for the treatment of hormone receptor (HR)-positive, human epidermal growth factor 2 (HER2)-negative, locally advanced, or metastatic breast cancer when used in combination with fulvestrant [97].

The synthesis of capivasertib (**12**) was originally reported by AstraZeneca [95]. As depicted in Scheme 12, (*S*)-3-amino-3-(4-chlorophenyl) propanoic acid (**101**) was reduced with BH_3 , yielding the desired primary amine **102**. In parallel, 4-chloro-7*H*-pyrrolo[2,3-*d*]pyrimidine (**103**) was subjected to a nucleophilic aromatic substitution with **104** in the presence of sodium carbonate to produce carboxylic acid derivative **105**. This was then coupled with primary amine **102**, in DMF using EDC and HOBT to form amide **106**. Finally, the Boc protecting group was removed from intermediate **106** under acidic conditions to yield capivasertib (**12**).

14. Nirogacestat (Ogsiveo™)

Nirogacestat (**13**, PF-03084014) is an oral, selective, reversible small molecule γ -secretase inhibitor [98] developed by SpringWorks Therapeutics, Inc. It is a chiral compound that contains a diamino-imidazole core heterocycle and a difluorotetralin fragment (Fig. 1). Prior to the discovery of PF-03084014, Pfizer synthesized a series of diamino-imidazole γ -secretase inhibitors, with **10a** (Fig. 11) being the most representative [99]. The IC_{50} for reducing amyloid- β (A β) in whole-cell assay of H4 APP_{Sw} cells is 0.4 nmol/L, while the IC_{50} for reducing A β in cell-free assay of human HeLa cells is 1.1 nmol/L.

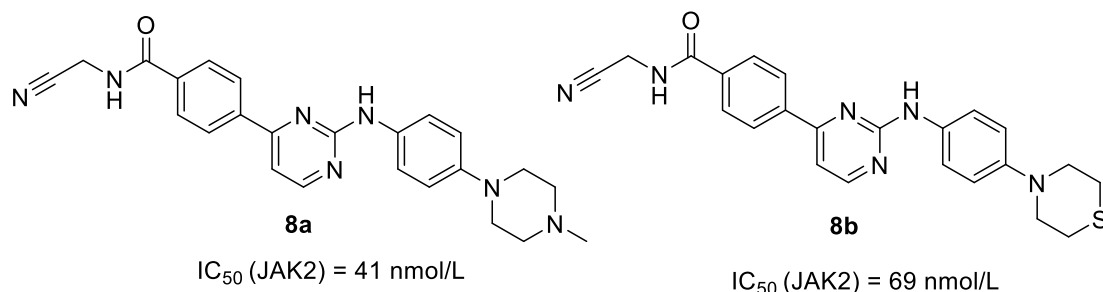
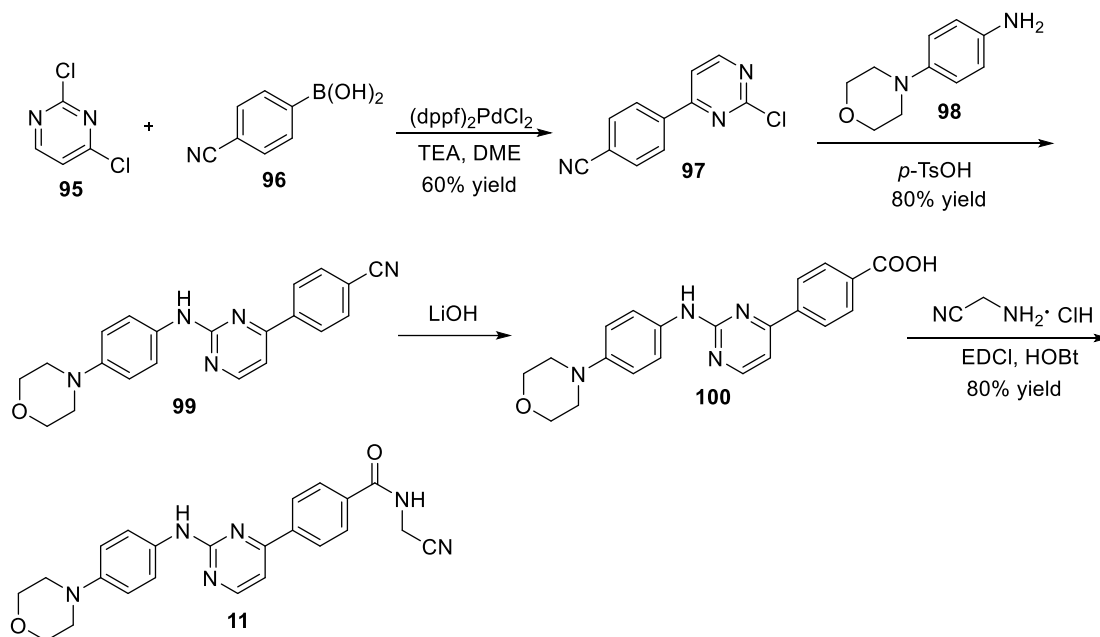


Fig. 9. Structures of **8a** and **8b**.



Scheme 11. Synthesis of Momelotinib (11).

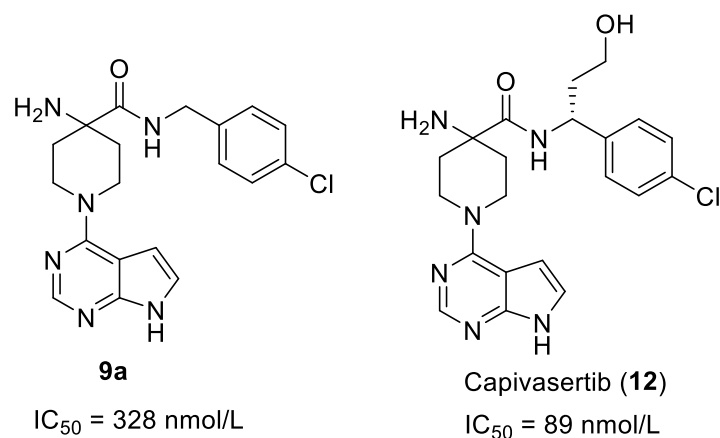


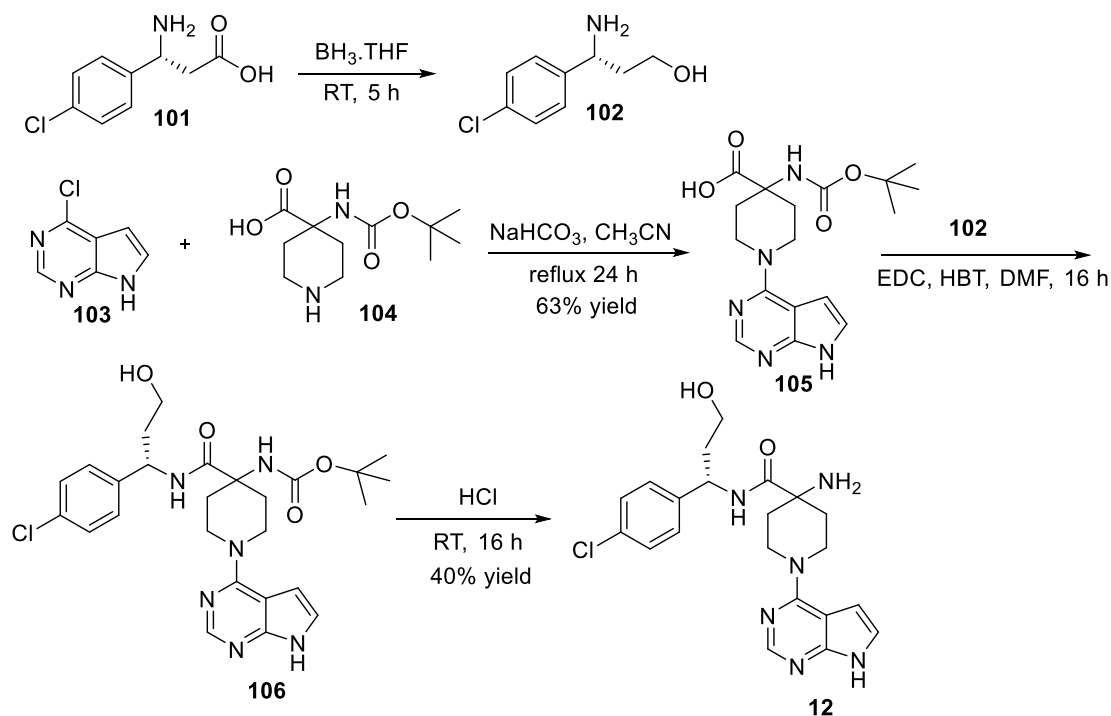
Fig. 10. Structures of 9a and capivasertib (12).

However, a single acute dose in vivo (guinea pigs) demonstrated a dose-dependent reduction in brain and plasma A β levels, with high plasma concentrations required for the brain A β -lowering effect negatively impacting the therapeutic index. Pfizer's subsequent SAR study on **10a** revealed that the introduction of the difluorotetralin group could reduce P-gp-mediated efflux, leading to the discovery of compound nirogacestat (**13**), which has a whole cell assay of H4 APP_{Sw} cells IC₅₀ of 1.2 nmol/L [100]. Nirogacestat (**13**) effectively reduced A β levels in the brain, cerebrospinal fluid, and plasma in a dose-responsive manner, while also mitigating A β and Notch-related side effects.

In adult patients with desmoid tumors, the median time to reach C_{max} was 1.5 h, while the time to achieve steady state was approximately 6 days. The mean C_{max} was recorded at 508 ng/mL, and the mean AUC was 3370 ng h/mL, with an absolute bioavailability of 19 %. Nirogacestat (**13**) is predominantly metabolized through N-dealkylation via CYP3A4 (accounting for 85 % of metabolism), along with contributions from other metabolic pathways involving CYP3A4, CYP2C19, CYP2C9, and CYP2D6. Phase III data from NCT03785964 [98] showed that the most common adverse events (AEs) were diarrhea (84 %), ovarian toxicity (in females of reproductive potential; 75 %). Prior to the advent

of pharmacological treatments, desmoid tumors were primarily managed through surgical intervention; however, the recurrence rate following surgical resection was as high as 77 %. The introduction of nirogacestat (**13**) has transformed this landscape, and it is now endorsed as a first-line treatment option in the National Comprehensive Cancer Network (NCCN) guidelines. Nirogacestat (**13**) was approved in the US FDA in November 2023 under the trade name Ogsiveo™ for adult patients with progressive desmoid tumors requiring systemic treatment [101].

The synthesis of nirogacestat (**13**) was originally reported by Pfizer [100]. In the process outlined in Scheme 13, the ester group in substituted nitroimidazole **107** was initially reduced to an aldehyde, followed by reductive alkylation with tert-butylamine to yield substituted nitroimidazole derivative **108**. Subsequent hydrogenation of 4-nitroimidazole on Pd/C led to the formation of the key diamino-imidazole intermediate **109**. Concurrently, the Friedel-Crafts reaction of 2-(2, 4-difluorophenyl)acetyl chloride (**110**) with ethylene produces tetralone **111**. A reductive alkylation reaction between tetralone **111** and (S)- norvaline *t*-butyl ester resulted in a diastereomeric mixture of amines, from which the desired diastereoisomer **112** was



Scheme 12. Synthesis of Capivasertib (12).

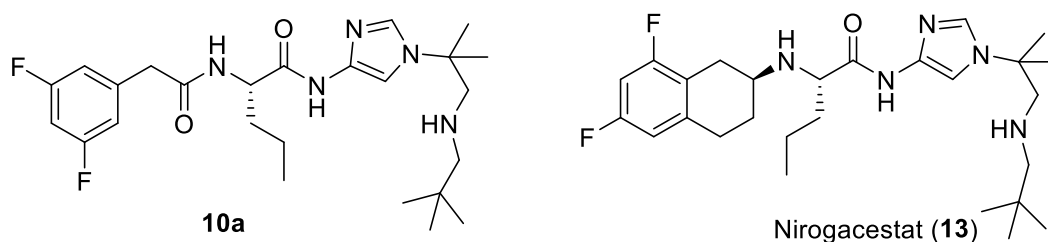
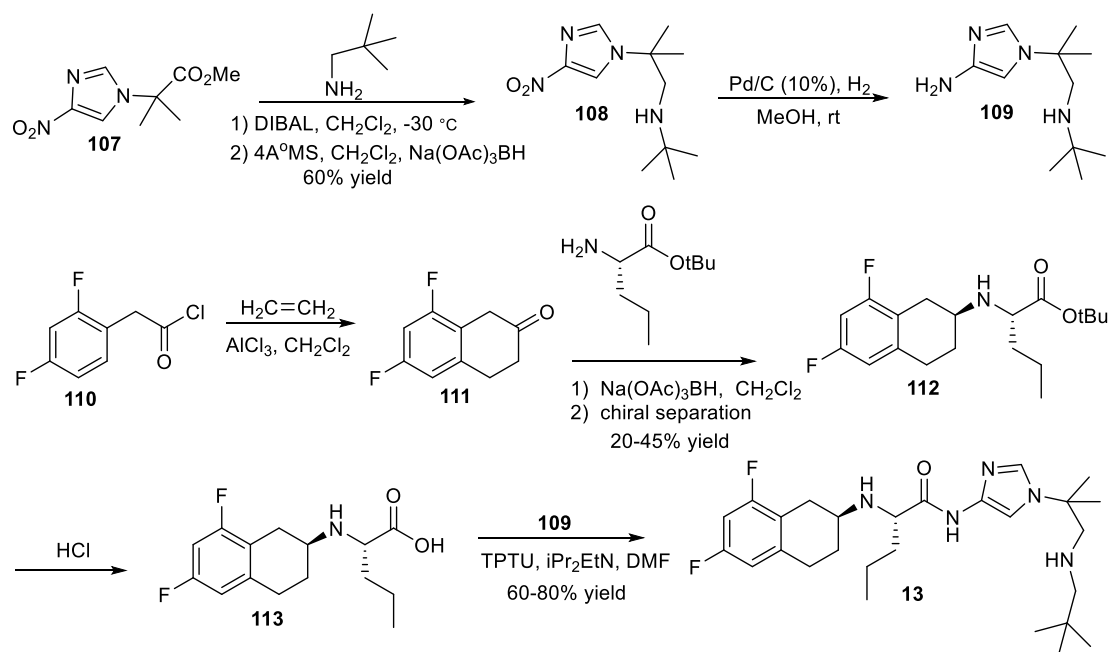


Fig. 11. Structures of 10a and nirogacestat (13).



Scheme 13. Synthesis of Nirogacestat (13).

separated using chiral HPLC. Acid catalysis was employed to hydrolyze ESTER intermediate **112** into acid **113**. The carboxyl group of intermediate **113** underwent condensation with aminoimidazole **109**, via activation by TPTU, ultimately yielding nirogacestat (**13**).

15. Conclusions and outlook

This article provides a comprehensive review of 13 newly developed nitrogen-containing heterocyclic drugs. These drugs include heterocyclic moieties such as pyridine (**5**), isoxazole (**2**, **8**), piperidine (**3**, **7**), pyrrolidine (**4**, **5**), and morpholine (**8**, **11**), pyrazole (**1**, **3**, **9**, **10**), imidazole (**8**, **13**), piperazine (**3**, **12**), pyrazine (**5**, **11**, **12**), triazole (**6**), and bisheterocyclic pyrrolo[2,3-*d*]pyrimidine (**7**, **12**). Among the small molecule drugs containing nitrogen heterocycles approved by FDA in the last 10 years, pyridine, piperidine occupy the first and second place, followed by pyrrolidine, piperazine, pyrimidine, indole respectively. Another noteworthy trend is the emergence of a large number of fused nitrogen heterocycles, which are mainly used for the treatment of cancer. With advancements in synthetic methods for nitrogen-containing compounds, the continued growth of nitrogen-containing heterocyclic drugs is anticipated.

Notably, over 50 % of the new drugs approved are chiral compounds like Jayprica™, Joenja™, Veozah™, Litfulo™, Zurzuva™, Truqap™, and Ogsiveo™. In the development of drugs, the conformation of chiral compounds greatly affects the therapeutic effect. However, the synthesis process of chiral compounds can be more complicated, which poses a challenge for us to select drugs for development in the future. Another area that needs attention is the toxicity of some drugs to special populations, such as the ovarian toxicity of the new drug nirogacestat (**13**), which poses another challenge to researchers subsequent to the development of safer and more effective nitrogen-containing heterocyclic compounds.

CRediT authorship contribution statement

Weijiang Luo: Writing – original draft. **Yiqi Liu:** Conceptualization. **Hui Qin:** Formal analysis. **Zeyan Zhao:** Software. **Suqi Wang:** Resources. **Weimin He:** Writing – review & editing. **Shengsong Tang:** Writing – review & editing, Formal analysis. **Junmei Peng:** Writing – review & editing, Conceptualization.

Declaration of competing interest

We have no known competing financial interests or personal relationships that could have appeared to influence the work reported in this paper.

Data availability

No data was used for the research described in the article.

Acknowledgments

We gratefully acknowledge the financial support from the Hunan Natural Science Foundation (2023JJ30525), Hunan Provincial Department of Education Scientific Research Project (22A0295), Hunan Province Key Laboratory for Antibody-based Drug and Intelligent Delivery System (2023-KL02) and Hunan Provincial Health Commission's 2023 Scientific Research Plan Topics (D202313057620).

References

- [1] A.K. Dhingra, B. Chopra, J.S. Dua, et al., Therapeutic potential of *N*-heterocyclic analogs as anti-inflammatory agents, *Antiinflamm Antiallergy Agents Med Chem* 16 (3) (2017) 136–152.
- [2] H. Liu, S. Long, K.P. Rakesh, et al., Structure-activity relationships (SAR) of triazine derivatives: promising antimicrobial agents, *Eur. J. Med. Chem.* 185 (2020) 111804.
- [3] D.K. Lang, R. Kaur, R. Arora, et al., Nitrogen-containing heterocycles as anticancer agents: an overview, *Anti Cancer Agents Med. Chem.* 20 (18) (2020) 2150–2168.
- [4] S. Chen, Y. Zhang, Y. Liu, et al., Highly efficient synthesis and Acaricidal and insecticidal activities of novel oxazolines with *N*-heterocyclic substituents, *J. Agric. Food Chem.* 69 (12) (2021) 3601–3606.
- [5] M. Muehlebach, A. Buchholz, W. Zambach, et al., Spiro *N*-methoxy piperidine ring containing arylidones for the control of sucking insects and mites: discovery of spiropidion, *Pest Manag. Sci.* 76 (10) (2020) 3440–3450.
- [6] L. Esquirol, T.S. Peat, E. Sugrue, et al., Bacterial catabolism of s-triazine herbicides: biochemistry, evolution and application, *Adv. Microb. Physiol.* 76 (2020) 129–186.
- [7] E. Vitaku, D.T. Smith, J.T. Njardarson, Analysis of the structural diversity, substitution patterns, and frequency of nitrogen heterocycles among U.S. FDA approved pharmaceuticals, *J. Med. Chem.* 57 (24) (2014) 10257–10274.
- [8] J. Akhtar, A.A. Khan, Z. Ali, et al., Structure-activity relationship (SAR) study and design strategies of nitrogen-containing heterocyclic moieties for their anticancer activities, *Eur. J. Med. Chem.* 125 (2017) 143–189.
- [9] K. Taruneshwar Jha, A. Shome, Chahat, et al., Recent advances in nitrogen-containing heterocyclic compounds as receptor tyrosine kinase inhibitors for the treatment of cancer: biological activity and structural activity relationship, *Bioorg. Chem.* 138 (2023) 106680.
- [10] G.L. Khatik, A.K. Datusalia, W. Ahsan, et al., A retrospect study on thiazole derivatives as the potential antidiabetic agents in drug discovery and developments, *Curr. Drug Discov. Technol.* 15 (3) (2018) 163–177.
- [11] G. Grover, R. Nath, R. Bhatia, et al., Synthetic and therapeutic perspectives of nitrogen containing heterocycles as anti-convulsants, *Bioorg. Med. Chem.* 28 (15) (2020) 115585.
- [12] R. Bai, C. Yao, Z. Zhong, et al., Discovery of natural anti-inflammatory alkaloids: potential leads for the drug discovery for the treatment of inflammation, *Eur. J. Med. Chem.* 213 (2021) 113165.
- [13] V. Antoci, D. Cucu, G. Zbancioc, et al., Bis-(imidazole/benzimidazole)-pyridine derivatives: synthesis, structure and antimycobacterial activity, *Future Med. Chem.* 12 (3) (2020) 207–222.
- [14] A. Koziol, E. Grela, K. Macegoniuk, et al., Synthesis of nitrogen-containing monoterpenoids with antibacterial activity, *Nat. Prod. Res.* 34 (8) (2020) 1074–1079.
- [15] D. Choudhary, B. Kumar, R. Kaur, Nitrogen-containing heterocyclic compounds: a ray of hope in depression? *Chem. Biol. Drug Des.* 103 (2) (2024) e14479.
- [16] D.D. Davis, Z. Ohana, H.M. Pham, Pirtobrutinib: a novel non-covalent BTK inhibitor for the treatment of adults with relapsed/refractory mantle cell lymphoma, *J. Oncol. Pharm. Pract.* 30 (1) (2024) 182–188.
- [17] J.R. Brown, S.M. Rothenberg, B.J. Brandhuber, et al., LOXO-305: targeting C481S Bruton tyrosine kinase in patients with ibrutinib-resistant CLL, *Blood* 134 (Supplement_1) (2019) 478, 478.
- [18] A.R. Mato, N.N. Shah, W. Jurczak, et al., Pirtobrutinib in relapsed or refractory B-cell malignancies (BRUIN): a phase 1/2 study, *Lancet* 397 (10277) (2021) 892–901.
- [19] S.J. Keam, Pirtobrutinib: first approval, *Drugs* 83 (6) (2023) 547–553.
- [20] D.A.J. Arguelles, C.T. Eary, J.W. Fennell, TW202225146 A1, 2022.
- [21] G. Cheng, CN116655538 A1, 2023.
- [22] A.W. Chiu, N. Bredenkamp, Sparsentan: a first-in-class dual endothelin and angiotensin II receptor antagonist, *Ann. Pharmacother.* (2023) 1–12.
- [23] N. Murugesan, Z. Gu, P.D. Stein, et al., Biphenylsulfonamide endothelin antagonists: structure-activity relationships of a series of mono- and disubstituted analogues and pharmacology of the orally active endothelin antagonist 2'-amino-*N*-(3,4-dimethyl-5-isoxazolyl)-4'-[(2-methylpropyl)[1, 1'-biphenyl]-2-sulfonamide (BMS-187308), *J. Med. Chem.* 41 (26) (1998) 5198–5218.
- [24] N. Murugesan, Z. Gu, L. Fadnis, et al., Dual angiotensin II and endothelin A receptor antagonists: synthesis of 2'-substituted *N*-3-isoxazolyl biphenylsulfonamides with improved potency and pharmacokinetics, *J. Med. Chem.* 48 (1) (2005) 171–179.
- [25] B.H. Rovin, J. Barratt, H.J.L. Heerspink, et al., Efficacy and safety of sparsentan versus irbesartan in patients with IgA nephropathy (PROTECT): 2-year results from a randomised, active-controlled, phase 3 trial, *Lancet* 402 (10417) (2023) 2077–2090.
- [26] Y.Y. Syed, Sparsentan: first approval, *Drugs* 83 (6) (2023) 563–568.
- [27] U. Ahmed, M.M. Saleem, M.A. Osman, et al., Novel FDA-approved zavegepant drug for treating migraine, *Ann Med Surg (Lond)* 86 (2) (2024) 923–925.
- [28] P.V. Chaturvedula, S.E. Mercer, S.S. Pin, et al., Discovery of (R)-*N*-(3-(7-methyl-1*H*-indazol-5-yl)-1-(4-(1-methylpiperidin-4-yl)-1-oxopropan-2-yl)-4-(2-oxo-1,2-dihydroquinolin-3-yl)piperidine-1-carboxamide (BMS-742413): a potent human CGRP antagonist with superior safety profile for the treatment of migraine through intranasal delivery, *Bioorg. Med. Chem. Lett.* 23 (11) (2013) 3157–3161.
- [29] A.P. Degnan, P.V. Chaturvedula, C.M. Conway, et al., Discovery of (R)-4-(8-fluoro-2-oxo-1,2-dihydroquinazolin-3(4*H*)-yl)-*N*-(3-(7-methyl-1*H*-indazol-5-yl)-1-oxo-1-(4-(piperidin-1-yl)piperidin-1-yl)propan-2-yl)piperidine-1-carboxamide (BMS-694153): a potent antagonist of the human calcitonin gene-related peptide receptor for migraine with rapid and efficient intranasal exposure, *J. Med. Chem.* 51 (16) (2008) 4858–4861.
- [30] R.B. Lipton, R. Croop, D.A. Stock, et al., Safety, tolerability, and efficacy of zavegepant 10 mg nasal spray for the acute treatment of migraine in the USA: a

- phase 3, double-blind, randomised, placebo-controlled multicentre trial, *Lancet Neurol.* 22 (3) (2023) 209–217.
- [31] S. Dhilon, Zavegeant: first approval, *Drugs* 83 (9) (2023) 825–831.
- [32] X. Han, R.L. Civiello, C.M. Conway, et al., The synthesis and SAR of calcitonin gene-related peptide (CGRP) receptor antagonists derived from tyrosine surrogates. Part 1, *Bioorg. Med. Chem. Lett.* 22 (14) (2012) 4723–4727.
- [33] X. Han, X.J. Jiang, R.L. Civiello, et al., Catalytic asymmetric syntheses of alpha-amino and alpha-hydroxyl acid derivatives, *J. Org. Chem.* 74 (10) (2009) 3993–3996.
- [34] B.E. Collins, J.L. Neul, Rett syndrome and MECP2 duplication syndrome: disorders of MECP2 dosage, *Neuropsychiatric Dis. Treat.* 18 (2022) 2813–2835.
- [35] C. Fu, D. Armstrong, E. Marsh, et al., Consensus guidelines on managing Rett syndrome across the lifespan, *BMJ Paediatr Open* 4 (1) (2020) e000717.
- [36] S.M. Kyle, N. Vashi, M.J. Justice, Rett syndrome: a neurological disorder with metabolic components, *Open Biol* 8 (2) (2018) 170216.
- [37] X.C. Lu, R.W. Chen, C. Yao, et al., NNZ-2566, a glypromate analog, improves functional recovery and attenuates apoptosis and inflammation in a rat model of penetrating ballistic-type brain injury, *J. Neurotrauma* 26 (1) (2009) 141–154.
- [38] I. Cacciatore, C. Cornacchia, L. Baldassarre, et al., GPE and GPE analogues as promising neuroprotective agents, *Mini Rev. Med. Chem.* 12 (1) (2012) 13–23.
- [39] D.G. Glaze, J.L. Neul, W.E. Kaufmann, et al., Double-blind, randomized, placebo-controlled study of trofinetide in pediatric Rett syndrome, *Neurol. Now.* 92 (16) (2019) e1912–e1925.
- [40] M. Darwish, J.M. Youakim, J. Harlick, et al., A phase 1, open-label study to evaluate the effects of food and evening dosing on the pharmacokinetics of oral trofinetide in healthy adult subjects, *Clin. Drug Invest.* 42 (6) (2022) 513–524.
- [41] J.L. Neul, A.K. Percy, T.A. Benke, et al., Trofinetide for the treatment of Rett syndrome: a randomized phase 3 study, *Nat. Med.* 29 (6) (2023) 1468–1475.
- [42] S.J. Keam, Trofinetide: first approval, *Drugs* 83 (9) (2023) 819–824.
- [43] C. Brewer M P, J.M. Shaw, J.A. Bonner, CN114667136 A, 2022.
- [44] V.K. Rao, S. Webster, V. Dalm, et al., Effective "activated PI3K δ syndrome"-targeted therapy with the PI3K δ inhibitor leniolisib, *Blood* 130 (21) (2017) 2307–2316.
- [45] K. Hoegenauer, N. Soldermann, F. Zecri, et al., Discovery of CDZ173 (leniolisib), representing a structurally novel class of PI3K delta-selective inhibitors, *ACS Med. Chem. Lett.* 8 (9) (2017) 975–980.
- [46] S. De Buck, K. Kucher, H. Hara, et al., CYP3A but not P-gp plays a relevant role in the in vivo intestinal and hepatic clearance of the delta-specific phosphoinositide-3 kinase inhibitor leniolisib, *Biopharm Drug Dispos.* 39 (8) (2018) 394–402.
- [47] V.K. Rao, S. Webster, A. Sediva, et al., A randomized, placebo-controlled phase 3 trial of the PI3K δ inhibitor leniolisib for activated PI3K δ syndrome, *Blood* 141 (9) (2023) 971–983.
- [48] S. Duggan, Z.T. Al-Salama, Leniolisib: first approval, *Drugs* 83 (10) (2023) 943–948.
- [49] N.G. Cooke, N. Graveleau, C. Hebach, CN102971317 A1, 2013.
- [50] G. Cheng, CN117534672 A1, 2024.
- [51] K. Skorupskaitė, J.T. George, R.A. Anderson, The kisspeptin-GnRH pathway in human reproductive health and disease, *Hum. Reprod. Update* 20 (4) (2014) 485–500.
- [52] H.R. Hoveyda, G.L. Fraser, G. Dutheil, et al., Optimization of novel antagonists to the neurokinin-3 receptor for the treatment of sex-hormone disorders (Part II), *ACS Med. Chem. Lett.* 6 (7) (2015) 736–740.
- [53] H. Depypere, C. Lademacher, E. Siddiqui, et al., Fezolinetant in the treatment of vasomotor symptoms associated with menopause, *Expet Opin. Invest. Drugs* 30 (7) (2021) 681–694.
- [54] G. Neal-Perry, A. Cano, S. Lederman, et al., Safety of fezolinetant for vasomotor symptoms associated with menopause: a randomized controlled trial, *Obstet. Gynecol.* 141 (4) (2023) 737–747.
- [55] A. Lee, Fezolinetant: first approval, *Drugs* 83 (12) (2023) 1137–1141.
- [56] H. Hoveyda, G. Dutheil, G. Fraser, WO2014154895 A1, 2014.
- [57] S. Eisman, R. Sinclair, Ritlecitinib: an investigational drug for the treatment of moderate to severe alopecia areata, *Expet Opin. Invest. Drugs* 30 (12) (2021) 1169–1174.
- [58] K. Ezzedine, E. Peeva, Y. Yamaguchi, et al., Efficacy and safety of oral ritlecitinib for the treatment of active nonsegmental vitiligo: a randomized phase 2b clinical trial, *J. Am. Acad. Dermatol.* 88 (2) (2023) 395–403.
- [59] W.J. Sandborn, S. Danese, J. Leszczyszyn, et al., Oral ritlecitinib and brepocitinib for moderate-to-severe ulcerative colitis: results from a randomized, phase 2b study, *Clin. Gastroenterol. Hepatol.* 21 (10) (2023) 2616–2628.
- [60] J. Wojciechowski, S.P. V. Y. Huh, et al., Evolution of ritlecitinib population pharmacokinetic models during clinical drug development, *Clin. Pharmacokinet.* 62 (12) (2023) 1765–1779.
- [61] Y. Tao, J.C. McWilliams, K.E. Wiglesworth, et al., Process development and scale up of a selective JAK3 covalent inhibitor PF-06651600, *Org. Process Res. Dev.* 23 (9) (2019) 1872–1880.
- [62] J. Liu, R. Solan, R. Wolk, et al., Evaluation of the effect of ritlecitinib on the pharmacokinetics of caffeine in healthy participants, *Br. J. Clin. Pharmacol.* 89 (7) (2023) 2208–2215.
- [63] B. King, J. Soung, C. Tziotziou, et al., Integrated safety analysis of ritlecitinib, an oral JAK3/TEC family kinase inhibitor, for the treatment of alopecia areata from the ALLEGRO clinical trial program, *Am. J. Clin. Dermatol.* 25 (2) (2024) 299–314.
- [64] H.A. Blair, Ritlecitinib: first approval, *Drugs* 83 (14) (2023) 1315–1321.
- [65] A. Garcia-Horton, K.W. Yee, Quizartinib for the treatment of acute myeloid leukemia, *Expet Opin. Pharmacother.* 21 (17) (2020) 2077–2090.
- [66] E. Estey, H. Döhner, Acute myeloid leukaemia, *Lancet* 368 (9550) (2006) 1894–1907.
- [67] Q. Chao, K.G. Sprankle, R.M. Grotzfeld, et al., Identification of N-(5-tert-butyl-isoxazol-3-yl)-N'-[4-[7-(2-morpholin-4-yl-ethoxy)imidazo[2,1-b][1,3]benzothiazol-2-yl]phenyl]urea dihydrochloride (AC220), a uniquely potent, selective, and efficacious FMS-like tyrosine kinase-3 (FLT3) inhibitor, *J. Med. Chem.* 52 (23) (2009) 7808–7816.
- [68] P.P. Zarrinkar, R.N. Gunawardane, M.D. Cramer, et al., AC220 is a uniquely potent and selective inhibitor of FLT3 for the treatment of acute myeloid leukemia (AML), *Blood* 114 (14) (2009) 2984–2992.
- [69] Z. Yu, J. Du, H. Hui, et al., LT-171-861, a novel FLT3 inhibitor, shows excellent preclinical efficacy for the treatment of FLT3 mutant acute myeloid leukemia, *Theranostics* 11 (1) (2021) 93–106.
- [70] K. Usuki, H. Handa, I. Choi, et al., Safety and pharmacokinetics of quizartinib in Japanese patients with relapsed or refractory acute myeloid leukemia in a phase 1 study, *Int. J. Hematol.* 110 (6) (2019) 654–664.
- [71] H.P. Erba, P. Montesinos, H.J. Kim, et al., Quizartinib plus chemotherapy in newly diagnosed patients with FLT3-internal-tandem-duplication-positive acute myeloid leukaemia (QuANTUM-First): a randomised, double-blind, placebo-controlled, phase 3 trial, *Lancet* 401 (10388) (2023) 1571–1583.
- [72] N. Alaa El-Deen, E. Dokla, M. Jaballah, et al., AML and FLT3: an update on FDA-approved or under review kinase inhibitors targeting FLT3 kinase, *Egypt. J. Chem.* 67 (2023) 529–553.
- [73] A.L. Althaus, M.A. Ackley, G.M. Belfort, et al., Preclinical characterization of zuranolone (SAGE-217), a selective neuroactive steroid GABA(A) receptor positive allosteric modulator, *Neuropharmacology* 181 (2020) 108333.
- [74] E. Engin, R.S. Benham, U. Rudolph, An emerging circuit pharmacology of GABA (A) receptors, *Trends Pharmacol. Sci.* 39 (8) (2018) 710–732.
- [75] G. Martinez Botella, F.G. Salituro, B.L. Harrison, et al., Neuroactive steroids. 2. 3 α -Hydroxy-3 β -methyl-21-(4-cyano-1H-pyrazol-1'-yl)-19-nor-5 β -pregnan-20-one (SAGE-217): a clinical next generation neuroactive steroid positive allosteric modulator of the (γ -Aminobutyric acid)(A) receptor, *J. Med. Chem.* 60 (18) (2017) 7810–7819.
- [76] S.V. Parikh, S.T. Aaronson, S.J. Mathew, et al., Efficacy and safety of zuranolone co-initiated with an antidepressant in adults with major depressive disorder: results from the phase 3 CORAL study, *Neuropsychopharmacology* 49 (2) (2024) 467–475.
- [77] K.M. Deligiannidis, S. Meltzer-Brody, B. Maximos, et al., Zuranolone for the treatment of postpartum depression, *Am. J. Psychiatr.* 180 (9) (2023) 668–675.
- [78] Y.A. Heo, Zuranolone: first approval, *Drugs* 83 (16) (2023) 1559–1567.
- [79] R.J. Pignolo, H. Wang, F.S. Kaplan, Fibrodysplasia ossificans progressiva (FOP): a segmental progeroid syndrome, *Front. Endocrinol.* 10 (2019) 908.
- [80] K.L. Wentworth, U. Masharani, E.C. Hsiao, Therapeutic advances for blocking heterotopic ossification in fibrodysplasia ossificans progressiva, *Br. J. Clin. Pharmacol.* 85 (6) (2019) 1180–1187.
- [81] O. Semler, M. Rehberg, N. Mehdi, et al., Current and emerging therapeutic options for the management of rare skeletal diseases, *Paediatr Drugs* 21 (2) (2019) 95–106.
- [82] S.M. Hoy, Palovarotene: first approval, *Drugs* 82 (6) (2022) 711–716.
- [83] R.J. Pignolo, G. Baujat, E.C. Hsiao, et al., Palovarotene for fibrodysplasia ossificans progressiva (FOP): results of a randomized, placebo-controlled, double-blind phase 2 trial, *J. Bone Miner. Res.* 37 (10) (2022) 1891–1902.
- [84] J.M. Lapiere, D.M. Rotstein, E.B. Sjogren, WO0228810 A2, 2002.
- [85] A. Tefferi, A. Pardanani, N. Gangat, Momelotinib (JAK1/JAK2/ACVR1 inhibitor): mechanism of action, clinical trial reports, and therapeutic prospects beyond myelofibrosis, *Haematologica* 108 (11) (2023) 2919–2932.
- [86] K. Ikeda, K. Ueda, Gaining MOMENTUM against anaemic myelofibrosis, *Lancet* 401 (10373) (2023) 248–249.
- [87] F. Passamonti, B. Mora, Myelofibrosis, *Blood* 141 (16) (2023) 1954–1970.
- [88] C.J. Burns, D.G. Bourke, L. Andraus, et al., Phenylaminopyrimidines as inhibitors of Janus kinases (JAKs), *Bioorg. Med. Chem. Lett.* 19 (20) (2009) 5887–5892.
- [89] J. Zheng, Y. Xin, J. Zhang, et al., Pharmacokinetics and disposition of momelotinib revealed a disproportionate human metabolite-resolution for clinical development, *Drug Metab. Dispos.* 46 (3) (2018) 237–247.
- [90] S. Verstovsek, A.T. Gerds, A.M. Vannucchi, et al., Momelotinib versus danazol in symptomatic patients with anaemia and myelofibrosis (MOMENTUM): results from an international, double-blind, randomised, controlled, phase 3 study, *Lancet* 401 (10373) (2023) 269–280.
- [91] S.J. Keam, Momelotinib: first approval, *Drugs* 83 (18) (2023) 1709–1715.
- [92] N.C. Turner, M. Oliveira, S.J. Howell, et al., Capivasertib in hormone receptor-positive advanced breast cancer, *N. Engl. J. Med.* 388 (22) (2023) 2058–2070.
- [93] S.J. Crabb, G. Griffiths, D. Dunkley, et al., Overall survival update for patients with metastatic castration-resistant prostate cancer treated with capivasertib and docetaxel in the phase 2 ProCAID clinical trial, *Eur. Urol.* 82 (5) (2022) 512–515.
- [94] T. Mchardy, J.J. Caldwell, K.M. Cheung, et al., Discovery of 4-amino-1-(7H-pyrrolo[2,3-d]pyrimidin-4-yl)piperidine-4-carboxamides as selective, orally active inhibitors of protein kinase B (Akt), *J. Med. Chem.* 53 (5) (2010) 2239–2249.
- [95] M. Addie, P. Ballard, D. Buttar, et al., Discovery of 4-amino-N-[(1S)-1-(4-chlorophenyl)-3-hydroxypropyl]-1-(7H-pyrrolo[2,3-d]pyrimidin-4-yl)piperidine-4-carboxamide (AZD5363), an orally bioavailable, potent inhibitor of Akt kinases, *J. Med. Chem.* 56 (5) (2013) 2059–2073.
- [96] C. Miller, R. Somavilla, D. Murphy, et al., The effect of food and acid-reducing agents on the pharmacokinetic profile of capivasertib: results from a randomized, crossover study, *Br. J. Clin. Pharmacol.* 89 (11) (2023) 3330–3339.
- [97] M. Shirley, Capivasertib: first approval, *Drugs* 84 (3) (2024) 337–346.

- [98] M. Gounder, R. Ratan, T. Alcindor, et al., Nirogacestat, a γ -secretase inhibitor for desmoid tumors, *N. Engl. J. Med.* 388 (10) (2023) 898–912.
- [99] M.A. Brodney, D.D. Auperin, S.L. Becker, et al., Diamide amino-imidazoles: a novel series of γ -secretase inhibitors for the treatment of Alzheimer's disease, *Bioorg. Med. Chem. Lett.* 21 (9) (2011) 2631–2636.
- [100] M.A. Brodney, D.D. Auperin, S.L. Becker, et al., Design, synthesis, and in vivo characterization of a novel series of tetralin amino imidazoles as γ -secretase inhibitors: discovery of PF-3084014, *Bioorg. Med. Chem. Lett.* 21 (9) (2011) 2637–2640.
- [101] S.J. Keam, Nirogacestat: first approval, *Drugs* 84 (3) (2024) 355–361.